

FEDCONCEPTEM: ROBUST FEDERATED LEARNING UNDER DIVERSE DISTRIBUTION SHIFTS

YongXin Guo

CUHK (SZ), P.R. China
yongxinguo@link.cuhk.edu.cn

Xiaoying Tang

CUHK (SZ), P.R. China
xiaoyingtang@cuhk.edu.cn

Tao Lin

Westlake University, P.R. China
lintao@westlake.edu.cn

ABSTRACT

Federated Learning (FL) is a machine learning paradigm that protects privacy by keeping client data on edge devices. However, optimizing FL in practice can be challenging due to the diversity and heterogeneity of the learning system. Recent research efforts have aimed to improve the optimization of FL with distribution shifts, but it is still an open problem how to train FL models when multiple types of distribution shifts, i.e., feature distribution skew, label distribution skew, and concept shift occur simultaneously.

To address this challenge, we propose a novel algorithm framework, FedConceptEM, for handling diverse distribution shifts in FL. FedConceptEM automatically assigns clients with concept shifts to different models, avoiding the performance drop caused by these shifts. At the same time, clients without concept shifts, even with feature or label skew, are assigned to the same model, improving the robustness of the trained models. Extensive experiments demonstrate that FedConceptEM outperforms other state-of-the-art cluster-based FL methods by a significant margin.

1 Introduction

Federated Learning (FL) is an emerging privacy-preserving distributed machine learning paradigm. The model is transmitted to the clients by the server, and when the clients have completed local training, the parameter updates are sent back to the server for integration. Clients are not required to provide local raw data during this procedure, maintaining their privacy. However, the non-IID nature of clients' local distribution hinders the performance of FL algorithms (McMahan et al., 2016; Li et al., 2018b; Karimireddy et al., 2020b; Li et al., 2021), and the distribution shifts among clients become a main challenge in FL.

Distribution shifts in FL. As identified in the seminal survey (Kairouz et al., 2021), three types of distribution shifts bottleneck the deployment of FL in practice (c.f. Figure 1):

- **Label distribution skew:** The marginal distributions of labels $\mathcal{P}(y)$ may vary across clients, even if the conditional distribution of features $\mathcal{P}(\mathbf{x}|y)$ is the same.
- **Feature distribution skew:** The marginal distribution of features $\mathcal{P}(\mathbf{x})$ may differ across clients, even if the conditional distribution of labels $\mathcal{P}(y|\mathbf{x})$ is shared.
- **Concept shift:** For tasks that use data \mathbf{x} to predict label y , the conditional distributions of labels $\mathcal{P}(y|\mathbf{x})$ may differ across clients, even if the marginal distributions of labels $\mathcal{P}(y)$ and features $\mathcal{P}(\mathbf{x})$ are shared.

However, current research in FL primarily focuses on addressing label distribution skew (Li et al., 2018b; Wang et al., 2020b; Karimireddy et al., 2020b), leaving the issues of feature distribution skew and concept shift among clients under-explored. Only a limited number of studies have investigated this issue in specific settings, either training robust feature extractors when train and test datasets have different feature distribution (Peng et al., 2019; Wang et al., 2022a; Shen et al., 2021), or addressing concept shifts under some specified conditions (Jothimurugesan et al., 2022). These attempts are far behind in addressing the challenges of the simultaneous occurrence of feature distribution, label distribution, and concept shifts among clients that naturally emerged in FL (as shown in Figure 1), due to the non-trivial **diverse distribution shift challenge**:



Figure 1: **Three types of distribution shifts in FL and our focus.** Different from prior works, we consider the challenge where clients meet all shifts: label skew, feature skew, and concept shift. E.g. client 1 has unbalanced labels, client 2 has drifting features, and client 3 has a shifted decision boundary due to concept shift.

we do not know if there exist distribution shifts among clients, as well as the type of these distribution shifts.

To this end, we propose our novel FedConceptEM framework as the first attempt in the field, a simple yet effective approach to train robust global models under diverse local distribution shifts. By leveraging the principle of soft clustering, FedConceptEM 1) assigns clients with only label and feature distribution skew to the same model, thereby improving the generalization ability of the trained models; and 2) assigns clients with concept shifts to different models, thus avoiding model performance drop. Such a design could further empower existing FL methods and facilitate learning in diverse and non-stationary environments.

We summarize our contributions below:

- We propose a novel soft-clustering-based algorithm framework—FedConceptEM—to address the diverse distribution shifts problem in FL.
- FedConceptEM is superior to other SOTA clustered FL algorithms, as justified by extensive empirical results on various datasets (FashionMNIST, CIFAR10, and CIFAR100) and neural architectures (CNN, MobileNetV2, and ResNet18).
- The FedConceptEM framework allows flexible yet effective extensions, including but not limited to, personalization, enhanced interpretability, integrating privacy-preserving techniques, and being adaptive to the number of clusters.

2 Related Works

Federated Learning with label and feature distribution shifts. As the de facto FL algorithm, McMahan et al. (2016); Lin et al. (2020) proposes to use local SGD to reduce communication bottlenecks, but non-IID data distribution among clients hinders performance (Li et al., 2018c; Wang et al., 2020b; Karimireddy et al., 2020b,a; Guo et al., 2021; Jiang & Lin, 2023). Addressing distribution shifts is a key problem in FL, while most existing works focusing on label distribution skew through techniques such as training robust global models (Li et al., 2018c, 2021) or variance reduction methods (Karimireddy et al., 2020b,a). As another line of research, studies about feature distribution skew in FL mostly focus on domain generalization to train models that can generalize to unseen feature distributions (Peng et al., 2019; Wang et al., 2022a; Shen et al., 2021; Sun et al., 2022; Gan et al., 2021). All of the above methods aim to train a single robust model. However, using a single model cannot solve the diverse distribution shift challenge, as the decision boundary changes when concept shifts occur.¹

Federated Learning with concept shifts. Concept shift is not a well-studied problem in FL. However, some special cases become an emerging topic recently. For example, research has shown that label noise can negatively impact model performance (Ke et al., 2022). Additionally, methods have been proposed to correct labels that have been corrupted

¹More detailed discussions can be found in Appendix C.

by noise (Fang & Ye, 2022; Xu et al., 2022). Recently, Jothimurugesan et al. (2022) also investigate the concept shift problem under the assumption that clients do not have concept shifts at the beginning of the training. However, it is difficult to ensure the non-existence of concept shifts when information about local distributions is not available in practice. Additionally, Jothimurugesan et al. (2022) did not address the issue of label and feature distribution skew. In this work, we consider a more realistic but more challenging scenario where clients could have all three kinds of shifts with each other, unlike Jothimurugesan et al. (2022) that needs to restrict the non-occurrence of concept shift at the initial training phase.

Clustered Federated Learning. Clustered Federated Learning (clustered FL) is a technique that groups clients into clusters based on their local data distribution to address the distribution shift problem. Various methods have been proposed for clustering clients, including using local loss values (Ghosh et al., 2020), communication time/local calculation time (Wang et al., 2022c), fuzzy c -Means (Stallmann & Wilbik, 2022), and hierarchical clustering (Zhao et al., 2020; Briggs et al., 2020; Sattler et al., 2020a). Some approaches, such as FedSoft (Ruan & Joe-Wong, 2022), combine clustered FL with personalized FL by allowing clients to contribute to multiple clusters. Other methods, such as FeSEM (Xie et al., 2020) and FedEM (Marfoq et al., 2021), use an Expectation-Maximization approach and maximize the log-likelihood objective function. Our proposed method, FedConceptEM, overcomes the drawbacks of FedEM and shows strong performance over other clustered FL methods.

3 Motivation: Mixture of Models Pave the Way for Learning Under Diverse Distribution Shifts

We outline the problem we studied in this work. On the one hand, we would like to train different models for clients that have concept shifts to avoid the performance drop, as evaluated in Ke et al. (2022). On the other hand, we would like to train all the clients without concept shifts on the same model. This design choice can be justified by some recent studies (Muandet et al., 2013; Li et al., 2018a; Wang et al., 2022b), where training data with feature and label distribution shift together will avoid the *spurious correlation* problem and thus improve the robustness of trained models.

Clustered FL is a technique to address distribution shifts among clients by dividing them into different clusters. Along with this line of research, in this work, we investigate the mixture of models problem and present a new clustered FL method as the solution. Therefore, the key becomes identifying the **rule for clustering**:

*separating clients with concept shifts into different models, while keeping clients without concept shifts in the same model.*²

In the following parts of this paper, we first introduce the Expectation Maximization (EM) algorithm, a well-known way for the mixture of models problem (Marfoq et al., 2021; Xie et al., 2020). Due to their limitations when dealing with the **rule for clustering**, we give our novel solutions, termed as FedConceptEM in Section 5. Furthermore, we discussed how to decide the number of clusters in FedConceptEM, and design an adaptive FedConceptEM method in Section 8.

4 Introduction to EMs and Their Limitations

In this section, we first introduce the EM algorithm and then show existing EM algorithm fails when considering the **rule for clustering**.

4.1 A Potential Idea: Expectation-Maximization (EM)

The Expectation-Maximization (EM) method is a powerful tool for solving mixture distribution problems and can be used for soft clustering by assuming data come from K underlying distributions and learning the weights of each data assigned to those distributions. A mixture distribution is a linear combination of K different distributions, given by,

$$\mathcal{P}(\mathbf{x}, y) = \sum_{k=1}^K \omega_k \mathcal{P}_k(\mathbf{x}, y; \theta_k), \quad (1)$$

where (\mathbf{x}, y) is a sample-pair of \mathcal{D} , $\mathcal{P}_k(\mathbf{x}, y; \theta_k)$ is probability of (\mathbf{x}, y) on the distribution that parameterized by θ_k , and ω_k is the weight assigned to this distribution.

²This paper examines the training of robust global models as a first step. Other enhancements to the FedConceptEM can be achieved by combining it with other methods in FL, such as personalized or hierarchical clustered FL, as discussed in section 9.

We present a generalized objective function of the Expectation-Maximization (EM) algorithm below³. Given M data sources $\{\mathcal{D}_1, \dots, \mathcal{D}_M\}$, where each local data distribution D_i is a mixture of K underlying distributions, the objective function of EM (Nguyen et al., 2020) maximizes the following log-likelihood function:

$$\mathcal{L}(\Theta, \Omega) := \frac{1}{N} \sum_{i=1}^M \sum_{j=1}^{N_i} \ln(\mathcal{P}(\mathbf{x}_{i,j}, y_{i,j})) + \sum_{i=1}^M \lambda_i \left(\sum_{k=1}^K \omega_{i,k} - 1 \right), \quad (2)$$

where $N_i := |\mathcal{D}_i|$, and $N = \sum_{i=1}^M N_i$. $(\mathbf{x}_{i,j}, y_{i,j})$ is the j -th data sampled from dataset D_i , and we assume that each data pair $(\mathbf{x}_{i,j}, y_{i,j})$ is drawn from the mixture distribution $\mathcal{P}(\mathbf{x}_{i,j}, y_{i,j})$ defined in (1). Note that $\Theta := [\theta_1, \dots, \theta_K]$ and $\Omega := [\omega_{0;0}, \dots, \omega_{0;K}, \dots, \omega_{M;K}] \in \mathbb{R}^{MK}$ are the parameters of the objective function $\mathcal{L}(\Theta, \Omega)$. λ_i is a Lagrange Multiplier of \mathcal{D}_i that enforces $\sum_{k=1}^K \omega_{i,k} = 1$.

The exact optimization procedure of the EM algorithm is defined by performing E-step and M-step alternatively (Marfoq et al., 2021), detailed as follows (for a given iterate t).

E-step:

$$\gamma_{i,j;k}^t = \frac{\omega_{i,k}^{t-1} \exp(-f_{i,k}(\mathbf{x}_{i,j}, y_{i,j}, \theta_k))}{\sum_{n=1}^K \omega_{i,n}^{t-1} \exp(-f_{i,n}(\mathbf{x}_{i,j}, y_{i,j}, \theta_n))}. \quad (3)$$

M-step:

$$\omega_{i,k}^t = \frac{1}{N_i} \sum_{j=1}^{N_i} \gamma_{i,j;k}^t, \quad (4)$$

$$\theta_k^t = \theta_k^{t-1} - \frac{\eta}{N} \sum_{i=1}^M \sum_{j=1}^{N_i} \gamma_{i,j;k}^t \nabla_{\theta} f_{i,k}(\mathbf{x}_{i,j}, y_{i,j}, \theta_k^{t-1}), \quad (5)$$

where $f_{i,k}(\mathbf{x}, y, \theta_k) \propto -\ln \mathcal{P}_k(y|\mathbf{x}; \theta_k)$ is the cross-entropy loss (Marfoq et al., 2021).

Remark 4.1 (Property of $\gamma_{i,j;k}$). We can observe from (5) that $\gamma_{i,j;k}$ can serve as the weight of data point $(\mathbf{x}_{i,j}, y_{i,j})$ that contributes to the update of θ_k , and $\omega_{i,k}$ is the average of $\gamma_{i,j;k}$ over all data points $(\mathbf{x}_{i,j}, y_{i,j})$ in D_i .

4.2 The Pitfalls of Existing EM Based Algorithms

The traditional EM algorithm, which maximizes the log-likelihood function $\mathcal{L}(\Theta, \Omega)$ as stated in (2), has been successful in various applications. However, it has limitations in our challenging scenario. As demonstrated in Figure 3, traditional EM algorithms may struggle to accurately assign data with concept shifts to different models. This can lead to a poor conditional distribution $\mathcal{P}_k(y|\mathbf{x}; \theta_k)$, which negatively impacts classification performance. The pitfalls of traditional EM are further supported by examples of more complex scenarios stated below.

Examples on complex scenarios. As our target is to deal with heterogeneous local distribution problem in FL, we construct a more realistic scenario with 100 clients and use FedEM (Marfoq et al., 2021) as a natural way that adapts traditional EM algorithm with local SGD in FL settings. In Figure 2(a), we show the distribution of $\gamma_{i,j;k}$ in FedEM as an illustration of the clustering results. However, we found that FedEM failed to assign data with concept shifts to different models, resulting in poor performance (see Table 1). We also identify that the clustering of FedEM is dominated by label distribution shift instead of concept shift in Appendix E.

5 ConceptEM as A Remedy for EM

In this section, we introduce a novel algorithm—termed as ConceptEM—to remedy EM with pitfalls caused by various distribution shifts as identified in Section 4.2.

Design of ConceptEM. Similar to traditional EM algorithms, ConceptEM also maximizes the objective function $\mathcal{L}(\Theta, \Omega)$. As discussed in the **rule for clustering**, the expected objective function $\mathcal{L}(\Theta, \Omega)$ needs to satisfy the following properties: 1) $\mathcal{L}(\Theta, \Omega)$ is positively related to the likelihood function $\mathcal{P}_k(\mathbf{x}, y; \theta_k)$, as the ultimate goal of ConceptEM is to maximize the likelihood function; 2) $\mathcal{L}(\Theta, \Omega)$ should only be small when data with concept shift is

³Such formulation covers the scenario of multiple datasets and can be trivially applied to FL.

assigned to the same model. The objective function of ConceptEM can then be defined as:

$$\begin{aligned} \mathcal{L}(\Theta, \Omega) = & \frac{1}{N} \sum_{i=1}^M \sum_{j=1}^{N_i} \ln \left(\sum_{k=1}^K \omega_{i;k} \mathcal{I}_k(\mathbf{x}_{i,j}, y_{i,j}, \theta_k) \right) \\ & + \sum_{i=1}^M \lambda_i \left(\sum_{k=1}^K \omega_{i;k} - 1 \right), \end{aligned} \quad (6)$$

where

$$\mathcal{I}_k(\mathbf{x}, y, \theta_k) = \frac{\mathcal{P}_k(\mathbf{x}, y; \theta_k)}{\mathcal{P}_k(\mathbf{x}; \theta_k) \mathcal{P}_k(y; \theta_k)} = \frac{\mathcal{P}_k(y|\mathbf{x}; \theta_k)}{\mathcal{P}_k(y; \theta_k)}. \quad (7)$$

We can observe that the value of $\mathcal{I}_k(\mathbf{x}, y, \theta_k)$ will decrease only when concept shift detected:

- When concept shift occurs, i.e., the conditional distribution $\mathcal{P}_k(y|\mathbf{x}; \theta_k)$ decreases given the current parameters θ_k , then $\mathcal{I}_k(\mathbf{x}, y, \theta_k)$ will be reduced.
- When label or feature distribution skew occurs, or more precisely when $\mathcal{P}_k(y; \theta_k)$ or $\mathcal{P}_k(\mathbf{x}; \theta_k)$ decreases, then $\mathcal{I}_k(\mathbf{x}, y, \theta_k)$ will increase as it is negatively related to $\mathcal{P}_k(y; \theta_k)$ and $\mathcal{P}_k(\mathbf{x}; \theta_k)$.

Remark 5.1 (Difficulty on calculating $\mathcal{I}_k(\mathbf{x}, y, \theta_k)$ in practice). *Note that $\mathcal{I}_k(\mathbf{x}, y, \theta_k)$ cannot be directly evaluated in practice, and both $\mathcal{P}_k(y|\mathbf{x}; \theta_k)$ and $\mathcal{P}_k(y; \theta_k)$ need to be approximated. We address this issue in the next section, where we maximize (6) by using an approximation $\tilde{\mathcal{I}}_k(\mathbf{x}, y, \theta_k)$ in (9).*

5.1 E-M Steps of ConceptEM

Due to the intractable calculation of $\mathcal{I}_k(\mathbf{x}, y, \theta_k)$, we introduce $\tilde{\mathcal{I}}_k(\mathbf{x}, y, \theta_k)$ as an approximation of $\mathcal{I}_k(\mathbf{x}, y, \theta_k)$. We elaborate the refined definition of (6) below:

$$\begin{aligned} \mathcal{L}(\Theta, \Omega) = & \frac{1}{N} \sum_{i=1}^M \sum_{j=1}^{N_i} \ln \left(\sum_{k=1}^K \omega_{i;k} \tilde{\mathcal{I}}_k(\mathbf{x}_{i,j}, y_{i,j}, \theta_k) \right) \\ & + \sum_{i=1}^M \lambda_i \left(\sum_{k=1}^K \omega_{i;k} - 1 \right), \end{aligned} \quad (8)$$

where,

$$\tilde{\mathcal{I}}_k(\mathbf{x}, y, \theta_k) = \frac{\exp(-f(\mathbf{x}, y, \theta_k)) \frac{1}{N} \sum_{i=1}^M \sum_{j=1}^{N_i} \gamma_{i,j;k}}{\frac{1}{N} \sum_{i=1}^M \sum_{j=1}^{N_i} \mathbf{1}_{\{y_{i,j}=y\}} \gamma_{i,j;k}}. \quad (9)$$

The intuition behind using $\tilde{\mathcal{I}}_k(\mathbf{x}, y, \theta_k)$ as an approximation comes from:

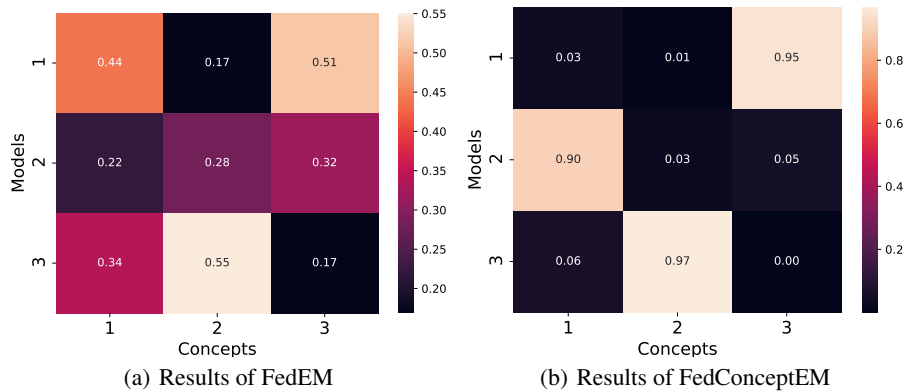


Figure 2: **Clustering results of FedEM and FedConceptEM.** We investigate the distribution of $\gamma_{i,j;k}$ using the CIFAR10 dataset and construct clients with three concepts (refer to Section 7.1 for more details). Our goal is to see how FedEM and FedConceptEM split clients into different models. We calculate the proportion of data with concept c assigned to θ_k for each (c, k) grid. Grids with different concepts show concept shifts. We find that FedEM’s distribution is chaotic and unrelated to concept shifts, while FedConceptEM clearly assigns concept shifted data to different models.

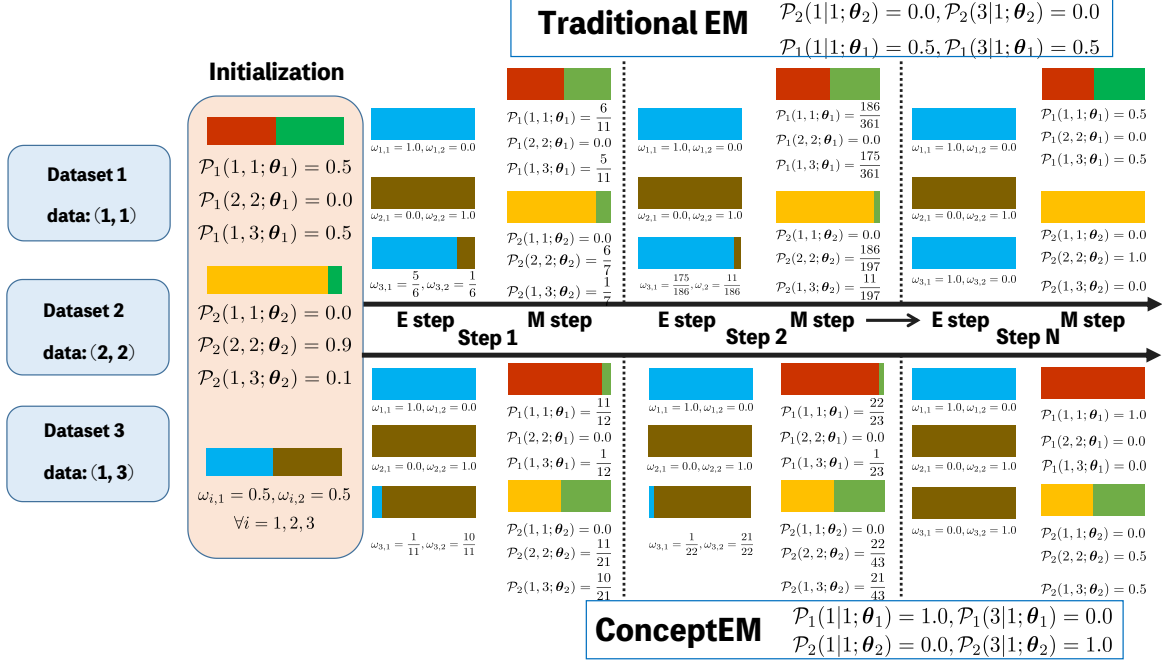


Figure 3: **Toy case for the pitfalls of traditional EM algorithms.** We create a simple example with three datasets that have an equal number of data points and compare results of traditional EM and ConceptEM. We show $\omega_{i,k}$ and $\mathcal{P}_k(\mathbf{x}, y; \theta_k)$ at each step, as well as the conditional distribution $\mathcal{P}(y|\mathbf{x})$ for classification tasks. Traditional EM has low classification results on dataset 1 and 3, but ConceptEM always finds a model θ_k where $\mathcal{P}_k(y|\mathbf{x}; \theta_k) = 1$ for all data in all datasets.

- The fact of $f(\mathbf{x}, y, \theta_k) \propto -\ln \mathcal{P}_k(y|\mathbf{x}; \theta_k)$. We can use $\exp(-f(\mathbf{x}, y, \theta_k))$ to approximate $\mathcal{P}_k(y|\mathbf{x}; \theta_k)$.
- The fact that $\gamma_{i,j,k}$ represents the weight of data $(\mathbf{x}_{i,j}, y_{i,j})$ assigned to θ_k in EM (c.f. Remark 4.1). Thus, $\frac{1}{N} \sum_{i=1}^M \sum_{j=1}^{N_i} \mathbf{1}_{\{y_{i,j}=y\}} \gamma_{i,j,k} / \frac{1}{N} \sum_{i=1}^M \sum_{j=1}^{N_i} \gamma_{i,j,k}$ corresponds to the proportion of data pairs labeled as y that choose model θ_k . This proportion can be used to approximate $\mathcal{P}_k(y; \theta_k)$.

We show in (12) that our proposed EM steps for ConceptEM—obtained by maximizing (8)—guarantee the same property of $\gamma_{i,j,k}$ as in traditional EM algorithms (c.f. Remark 4.1). This observation supports our intuition that $\tilde{\mathcal{I}}_k(\mathbf{x}, y, \theta_k)$ can approximate $\mathcal{I}_k(\mathbf{x}, y, \theta_k)$ while maximizing (8) using our proposed EM steps.

We elaborate on EM steps for ConceptEM below (proof details refer to Appendix A), where

E-step:

$$\gamma_{i,j,k}^t = \frac{\omega_{i,k}^{t-1} \tilde{\mathcal{I}}_k(\mathbf{x}_{i,j}, y_{i,j}, \theta_k^{t-1})}{\sum_{n=1}^K \omega_{i,n}^{t-1} \tilde{\mathcal{I}}_k(\mathbf{x}_{i,j}, y_{i,j}, \theta_k^{t-1})}. \quad (10)$$

M-step:

$$\omega_{i,k}^t = \frac{1}{N_i} \sum_{j=1}^{N_i} \gamma_{i,j,k}^t, \quad (11)$$

$$\theta_k^t = \theta_k^{t-1} - \eta \frac{1}{N} \sum_{i=1}^M \sum_{j=1}^{N_i} \gamma_{i,j,k}^t \nabla_{\theta} f_{i,k}(\mathbf{x}_{i,j}, y_{i,j}, \theta_k^{t-1}). \quad (12)$$

Experiments justify the benefits of ConceptEM over traditional EM. Firstly, from the toy case in Figure 3 we can observe that ConceptEM effectively assigns data with concept shifts to different models. We can see that for all data (\mathbf{x}, y) in the three datasets, there is always a model θ_k where $\mathcal{P}_1(y|\mathbf{x}; \theta_k) = 1.0$. This suggests that ConceptEM has better classification results compared to traditional EM.

Furthermore, we report the distribution of $\gamma_{i,j,k}$ after running FedConceptEM as the same setting in Section 4.2: FedConceptEM successfully assign data with concept shifts to different models (c.f. Figure 2(b)) and achieve significant performance gain over FedEM (as supported by Table 1).

Algorithm 1 FedConceptEM Algorithm Framework

Require: number of models K , initial parameters $\Theta^0 = [\theta_1^0, \dots, \theta_K^0]$, global learning rate η_g , initial weights $\omega_{i,k}^0 = \frac{1}{K}$ for any $i \leq M, k \leq K$, and $\gamma_{i,j;k} = \frac{1}{K}$ for any $i \leq M, j \leq N_i, k \leq K$, local learning rate η_l .

Ensure: trained parameters $\Theta^T = [\theta_1^T, \dots, \theta_K^T]$ and weights $\omega_{i,k}^T$ for any $i \leq M, k \leq K$.

```
1: for round  $t = 1, \dots, T$  do
2:   Adapted: Check & remove model via Algorithm 2.
3:   communicate  $\Theta^t$  to the chosen clients.
4:   for client  $i \in \mathcal{S}^t$  in parallel do
5:     initialize local model  $\theta_{i,k}^{t,0} = \theta_k^t, \forall k$ .
6:     Update  $\gamma_{i,j;k}^t$  by (10),  $\forall j, k$ .
7:     Update  $\omega_{i,k}^t$  by (11),  $\forall k$ .
8:     Local update  $\theta_{i,k}^{t,\mathcal{T}}$  by (13).
9:     communicate  $\Delta\theta_{i,k}^t \leftarrow \theta_{i,k}^{t,\mathcal{T}} - \theta_{i,k}^{t,0}, \forall k$ .
10:     $\Delta\theta_k^t \leftarrow \frac{\eta_g}{\sum_{i \in \mathcal{S}^t} N_i} \sum_{i \in \mathcal{S}^t} N_i \Delta\theta_{i,k}^t, \forall k$ .
11:     $\theta_k^{t+1} \leftarrow \theta_k^t + \Delta\theta_k^t, \forall k$ .
```

5.2 Convergence of ConceptEM

Assumption 1 (Smoothness Assumption). Assume local objective functions $f_{i,k}(\theta)$ are L -smooth, i.e. $\|\nabla f_{i,k}(\theta_1) - \nabla f_{i,k}(\theta_2)\| \leq L \|\theta_1 - \theta_2\|$.

Assumption 2 (Bounded Gradient Assumption). Assume that the gradient of local objective functions $\nabla f_{i,k}(\theta)$ are bounded, i.e. $\mathbb{E} [\|\nabla f_{i,k}(\theta)\|^2] = \frac{1}{N} \sum_{i=1}^M \sum_{j=1}^{N_i} \|\nabla f_{i,k}(\mathbf{x}_{i,j}, y_{i,j}, \theta)\|^2 \leq \sigma^2$.

The assumptions of smoothness (Assumption 1) and bounded gradient (Assumption 2) are commonly used in non-convex optimization problems (Chen et al., 2018; Mertikopoulos et al., 2020). We introduce the bounded gradient assumption here as we only assume $f_{i,k}(\theta)$ to be L -smooth, and $\mathcal{L}(\Theta, \Omega)$ may not be a smooth function. We prove that ConceptEM converges under these regular assumptions and achieves the standard $O(1/\epsilon)$ convergence rate⁴.

Theorem 5.2 (Convergence rate of ConceptEM). Assume $f_{i,k}$ satisfy Assumption 1-2, setting T as the number of iterations, and $\eta = \frac{8}{27L+9\sigma^2}$, we have,

$$\frac{1}{T} \sum_{t=0}^{T-1} \sum_{k=1}^K \|\nabla_{\theta_k} \mathcal{L}(\Theta^t, \Omega^t)\|^2 \leq \mathcal{O}\left(\frac{(27L+9\sigma^2)(\mathcal{L}^* - \mathcal{L}^0)}{4T}\right),$$

where \mathcal{L}^* is the upper bound of $\mathcal{L}(\Theta, \Omega)$, and $\mathcal{L}^0 = \mathcal{L}(\Theta^0, \Omega^0)$. Proof details refer to Appendix B.

6 FedConceptEM: Adapting ConceptEM into FL

In this section, we adapt ConceptEM into FL scenarios by incorporating local steps and client sampling to improve communication efficiency. The overall process is summarized in Algorithm 1. As shown in Algorithm 1, at the beginning of round t , server transmit parameters $\Theta^t = [\theta_1^t, \dots, \theta_K^t]$ to clients. Then clients first locally update $\gamma_{i,j;k}^{t+1}$ and $\omega_{i,k}^{t+1}$ by (10) and (11) respectively. Then clients initialize $\theta_{i,k}^{t,0} = \theta_k^t$, and update parameters $\theta_{i,k}^{t,\tau}$ for \mathcal{T} local steps:

$$\theta_{i,k}^{t,\tau} = \theta_{i,k}^{t,\tau-1} - \frac{\eta_l}{N_i} \sum_{j=1}^{N_i} \gamma_{i,j;k}^t \nabla_{\theta} f_{i,k}(\mathbf{x}_{i,j}, y_{i,j}, \theta_{i,k}^{t,\tau-1}), \quad (13)$$

where τ is the current local iteration, and η_l is the local learning rate. In our algorithm, the global aggregation step uses the FedAvg method as the default option. However, other global aggregation methods e.g. (Wang et al., 2020a,b) can be implemented if desired.

⁴The convergence analysis and techniques of ConceptEM can be trivially extended to FedConceptEM, by adding the component of performing local update steps.

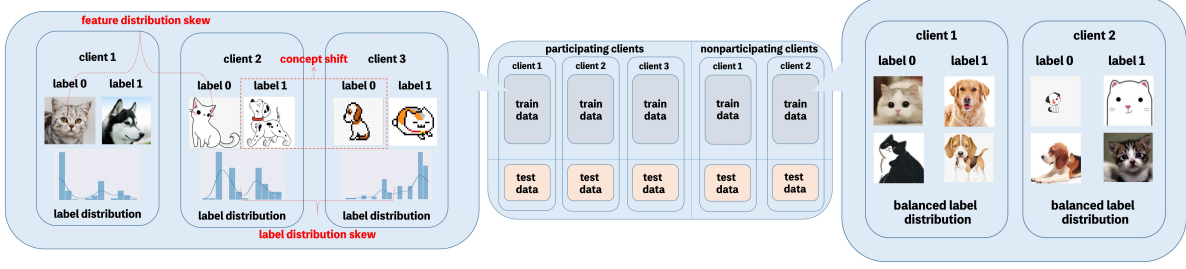


Figure 4: **Illustration of our numerical evaluation protocols.** Clients are divided into two categories: participating clients attend training and nonparticipating clients are used for testing. Both groups have IID train and test datasets. Participating clients simulate real-world scenarios and may have different label and feature distributions and concept shifts. Nonparticipating clients are used to testing model robustness. Labels on nonparticipating clients are swapped in the same way as participating clients for each concept.

Model prediction of FedConceptEM for supervised tasks. The model prediction of FedConceptEM for supervised tasks is performed using the same method as in FedEM Marfoq et al. (2021). I.e., given data \mathbf{x} for client i , the predicted label is calculated as $y_{\text{pred}} = \sum_{k=1}^K \omega_{i,k} \sigma(m_{i,k}(\mathbf{x}, \theta_k))$, where $m_{i,k}(\mathbf{x}, \theta_k)$ is the output of model θ_k given data \mathbf{x} , and σ is the softmax function. Note that the aforementioned $f_{i,k}(\mathbf{x}, y; \theta_k)$ is the cross entropy loss of $\sigma(m_{i,k}(\mathbf{x}, \theta_k))$ and y . When new clients join the system, they must first perform the E-step to obtain the optimal weights $\gamma_{i,j;k}$ and $\omega_{i,k}$ by (10) and (11) on their local train (or validation) datasets before proceeding to test.

Discussion: adding stochastic noise on $\gamma_{i,j;k}$ preserves client privacy. The $\mathcal{P}_k(y; \theta_k)$ in (9) uses the following term as an approximation

$$\frac{\frac{1}{N} \sum_{i=1}^M \sum_{j=1}^{N_i} \mathbf{1}_{\{y_{i,j}=y\}} \gamma_{i,j;k}}{\frac{1}{N} \sum_{i=1}^M \sum_{j=1}^{N_i} \gamma_{i,j;k}}, \quad (14)$$

where the collected $\sum_{j=1}^{N_i} \mathbf{1}_{\{y_{i,j}=y\}} \gamma_{i,j;k}$ from clients may leak the local label distributions. An additional zero-mean Gaussian noise can be added to tackle this issue:

$$C_{y,i} = c_{\xi_i} + \sum_{j=1}^{N_i} \mathbf{1}_{\{y_{i,j}=y\}} \gamma_{i,j;k}, \quad (15)$$

where $c_{\xi_i} \sim \mathcal{N}(0, \xi_i^2)$, and ξ_i is the standard deviation of the Gaussian noise of client i (which can chosen by clients). By definition of $C_y = 1/N \sum_{i=1}^M C_{y,i}$, we can find that

$$C_y := c_{\xi_g} + \frac{1}{N} \sum_{i=1}^M \sum_{j=1}^{N_i} (\mathbf{1}_{\{y_{i,j}=y\}} \gamma_{i,j;k} + \xi_i^2 / N^2), \quad (16)$$

where $c_{\xi_g} \sim \mathcal{N}(0, \sum_{i=1}^M \xi_i^2 / N^2)$, and the standard deviation of $\mathcal{N}(0, \sum_{i=1}^M \xi_i^2 / N^2)$ decreases as N increases. Therefore, when there is a large number of clients, we can obtain a relatively precise $C_y \approx \frac{1}{N} \sum_{i=1}^M \sum_{j=1}^{N_i} \mathbf{1}_{\{y_{i,j}=y\}} \gamma_{i,j;k}$ without accessing the true $\sum_{j=1}^{N_i} \mathbf{1}_{\{y_{i,j}=y\}} \gamma_{i,j;k}$. Note that the performance of FedConceptEM will not be significantly affected by the magnitude of noise, as justified in Figure 5(a).

7 Numerical Results

In this section, we show the superior performance of FedConceptEM compared with other FL baselines on FashionM-NIST, CIFAR10, and CIFAR100 datasets.

7.1 Experiment Settings

We introduce the considered evaluation settings below (and see Figure 4); more details about hyper-parameter settings, datasets, and algorithms can be found in Appendix D.5.

Table 1: **Performance of algorithms over various datasets and neural architectures.** We evaluated the performance of our algorithms using the FashionMNIST, CIFAR10 and CIFAR100 datasets split into 300 clients. We initialized 3 models for clustered FL methods and reported mean local and global test accuracy on the round that achieved the best train accuracy for each algorithm. We report FedConceptEM-FT by fine-tuning FedConceptEM for one local epoch; “CFL (3)” refers to restricting the number of models in CFL (Sattler et al., 2020b) to 3. We highlight the best and the second best results for each of the two main blocks, using **bold font** and **blue text**.

Algorithm	FashionMNIST (CNN)		CIFAR10 (MobileNetV2)		CIFAR100 (MobileNetV2)	
	Local	Global	Local	Global	Local	Global
FedAvg	42.12 \pm 0.33	34.35 \pm 0.92	30.28 \pm 0.38	30.47 \pm 0.76	12.72 \pm 0.82	10.53 \pm 0.57
IFCA	47.90 \pm 0.60	31.30 \pm 2.69	43.76 \pm 0.40	26.62 \pm 3.34	17.46 \pm 0.10	9.12 \pm 0.78
CFL	42.47 \pm 0.02	32.37 \pm 0.09	67.14 \pm 0.87	26.19 \pm 0.26	52.90 \pm 1.48	1.65 \pm 0.96
CFL (3)	41.77 \pm 0.40	33.53 \pm 0.35	41.49 \pm 0.64	29.12 \pm 0.02	26.36 \pm 0.33	7.15 \pm 1.10
FeSEM	60.99 \pm 1.01	47.63 \pm 0.99	45.32 \pm 0.16	30.79 \pm 0.02	18.46 \pm 3.96	9.76 \pm 0.64
FedEM	56.64 \pm 2.14	28.08 \pm 0.92	51.31 \pm 0.97	43.35 \pm 2.29	17.95 \pm 0.08	9.72 \pm 0.22
FedConceptEM	66.51 \pm 2.39	59.00 \pm 4.91	62.74 \pm 2.37	63.83 \pm 2.26	21.64 \pm 0.33	18.72 \pm 1.90
local	92.79 \pm 0.58	12.92 \pm 4.93	82.71 \pm 0.25	10.59 \pm 0.69	86.58 \pm 0.08	1.00 \pm 0.18
pFedMe	93.13 \pm 0.32	14.77 \pm 3.39	82.63 \pm 0.05	9.87 \pm 0.85	86.83 \pm 0.23	1.20 \pm 0.04
APFL	93.29 \pm 0.16	33.40 \pm 0.89	85.03 \pm 0.54	27.57 \pm 2.50	88.09 \pm 0.13	8.52 \pm 0.73
FedSoft	91.35 \pm 0.04	19.88 \pm 0.50	83.08 \pm 0.02	22.00 \pm 0.50	85.80 \pm 0.29	1.85 \pm 0.21
FedConceptEM-FT	91.02 \pm 0.26	62.37 \pm 1.09	82.81 \pm 0.90	65.33 \pm 1.80	87.14 \pm 0.39	16.27 \pm 0.09

Table 2: **Performance of algorithms on ResNet18.** We evaluated the performance of our algorithms on the CIFAR10 and CIFAR100, which were split into 100 clients, and initialize 3 models for clustered FL methods. We report the mean local test accuracy and global test accuracy on the round that achieves the best train accuracy for each algorithm.

Algorithm	CIFAR10		CIFAR100	
	Local	Global	Local	Global
FedAvg	25.58	26.10	13.48	12.87
IFCA	31.90	10.47	18.34	12.00
CFL	26.06	24.53	13.94	12.60
CFL (3)	25.18	24.80	13.34	12.13
FeSEM	34.56	21.93	17.28	12.90
FedEM	41.28	34.17	25.82	24.77
FedConceptEM	49.16	47.80	31.76	28.10

Evaluation and datasets. We construct two client types: participating clients and nonparticipating clients (detailed in Figure 4), and report the 1) *local accuracy*: the mean test accuracy of participating clients; 2) *global accuracy*: the mean test accuracy of nonparticipating clients.

- **Participating clients:** We construct the scenario that contains the issues of label skew, feature skew, and concept shift. For label skew, we use the idea introduced in Yurochkin et al. (2019); Hsu et al. (2019); Reddi et al. (2021), where we leverage the Latent Dirichlet Allocation (LDA) with parameter $\alpha = 1.0$. For feature skew, we utilize the idea of constructing FashionMNIST-C (Weiss & Tonella, 2022), CIFAR10-C, and CIFAR100-C (Hendrycks & Dietterich, 2019). For the concept shift, we change the labels of partial clients (i.e. from y to $(C - y)$, where C is the number of classes). Unless mentioned otherwise we assume only three concepts exist in the learning.
- **Nonparticipating clients:** We use the original test datasets of FashionMNIST, CIFAR10, and CIFAR100. To evaluate the ability of algorithms to handle concept shifts, we create three non-participating clients with balanced label distribution for each dataset. The labels for these non-participating clients will be swapped in the same way as the participating clients for each concept.

Baseline algorithms. We choose FedAvg (McMahan et al., 2016) as an example in traditional FL. For clustered FL methods, we choose IFCA (Ghosh et al., 2020), CFL (Sattler et al., 2020b), FeSEM (Xie et al., 2020), and FedEM (Marfoq et al., 2021). We also include some personalized FL methods, including pFedMe (T Dinh et al., 2020), APFL (Deng et al., 2020), and FedSoft (Ruan & Joe-Wong, 2022) to show the robustness of FedConceptEM and the potential of FedConceptEM on combining with them.

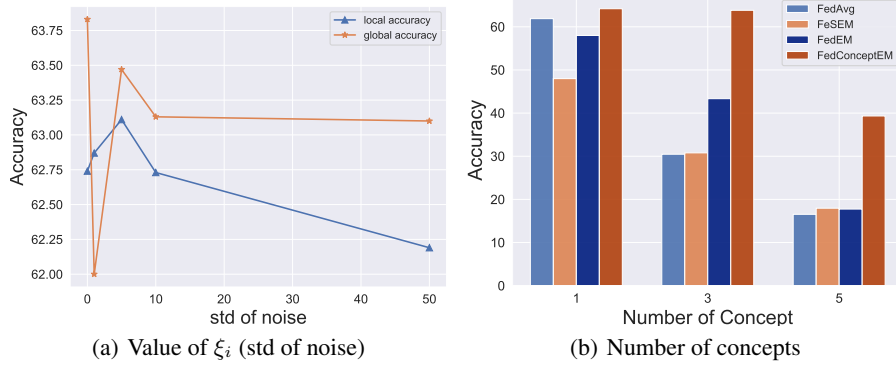


Figure 5: **Ablation study on the value of noise and the number of concepts.** We report the local & global test accuracy on the CIFAR10 for the round that achieves the best training accuracy for each trial. Figure 5(a) shows FedConceptEM’s local and global accuracies with different noise std values. Figure 5(b) shows clustered FL’s global accuracy with varying numbers of concepts. We use [3, 3, 5] models for the scenarios with [1, 3, 5] concepts.

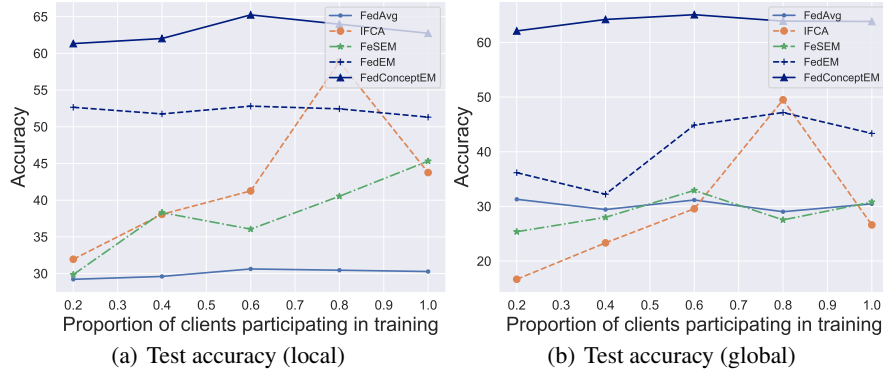


Figure 6: **Ablation study on the number of participation clients in each round.** We report the local & global test accuracies on the CIFAR10 for the round that achieves the best training accuracy.

7.2 Results

Superior performance of FedConceptEM over other strong FL baselines. The results in Table 1 and Table 2 demonstrate that: i) FedConceptEM consistently achieves significantly higher global accuracy compared to other FL baselines. ii) FedConceptEM performs better in terms of local accuracy compared to most other clustered FL methods, except for CFL. However, models trained using CFL and CFL (3) have the lowest global accuracy among all clustered FL methods, indicating their poor robustness on unseen global distributions. iii) CFL (3) is a variant that restricts the number of models of CFL to the exact number of concepts (i.e. 3), and we can observe that the local accuracy of CFL (3) is not significantly better than other clustered FL methods. iv) Personalized FL methods struggle to generalize to global distributions, in contrast to the FedConceptEM-FT—constructed by fine-tuning FedConceptEM for one local epoch—can achieve comparable performance with personalized FL methods on local accuracy while maintaining the high global performance.

FedConceptEM is robust to stochastic noise when preserving privacy. In (16) of Section 6, we show performance of FedConceptEM by incorporating random noise sampled from $\mathcal{N}(0, \xi_i)$ to enhance privacy. Figure 5(a) shows that increasing the value of ξ_i to 50 does not significantly affect the performance of FedConceptEM (about 1% performance drop), and will also outperform other methods.

FedConceptEM is robust to the client participation ratio in each communication round. Figure 6 demonstrates how the number of clients participating in training in each communication round impacts the performance of different

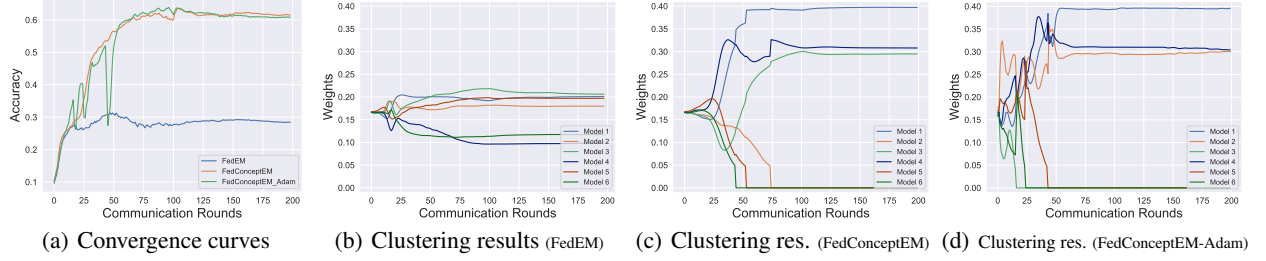


Figure 7: **Adaptive process of FedConceptEM.** We split CIFAR10 dataset into 300 clients, initialize 6 models, and report the global accuracy per round for the convergence result. We also show the clustering results by calculating weights by $\sum_{i,j} \gamma_{i,j;k} / \sum_{i,j,k} \gamma_{i,j;k}$, representing the proportion of clients that select model k . We use $\delta = 0.05$ here. Ablation study on δ refers to Appendix E.2.

algorithms. Our results show that the performance of FedConceptEM is more robust to variations in the number of participating clients compared to other methods⁵.

Performance gain of FedConceptEM increase as the number of concepts increase. In Figure 5(b), we see that: 1) FedConceptEM has a higher global accuracy compared to other methods, and this advantage becomes more pronounced as the number of concepts increases; 2) When clients have only one concept, using multiple models (such as FedEM and FeSEM) does not perform as well as using a single model (FedAvg). However, FedConceptEM is still better than FedAvg and maintains robustness.

8 Discussion: Adaptive FedConceptEM

In previous sections, the algorithm design assumes a fixed number of models with the equivalence to the number of concepts. However, in reality, the number of concepts may be unknown. This section explores how to adaptively determine the number of models when the number of concepts is uncertain.

8.1 Adaptive Concept Numbers in FedConceptEM

In this subsection, we demonstrate that FedConceptEM effectively groups clients without concept changes into the same models, aiding in identifying the number of concepts. We will begin by explaining the phenomenon, then we give practical examples using real datasets.

Intuition. FedConceptEM can avoid “bad cases” of clustering dominated by label skew and feature skew, i.e., $\mathcal{P}_k(y; \theta_k)$ or $\mathcal{P}_k(\mathbf{x}; \theta_k)$ varies among models. Considering data with label y_1 or data \mathbf{x}_1 such that $\mathcal{P}_k(y_1; \theta_k)$ or $\mathcal{P}_k(\mathbf{x}_1; \theta_k)$ is small. Then in the next E-step of FedConceptEM (c.f. (10)), due to the negative relation of $\tilde{\mathcal{I}}(\mathbf{x}, y, \theta_k)$ to both $\mathcal{P}_k(y_1; \theta_k)$ and $\mathcal{P}_k(\mathbf{x}_1; \theta_k)$, data with label y_1 or feature \mathbf{x}_1 will assign larger weights to model θ_k , resulting in an increase of $\mathcal{P}_k(y_1; \theta_k)$ and $\mathcal{P}_k(\mathbf{x}_1; \theta_k)$.

Experiments on CIFAR10. We conduct experiments on CIFAR10 using the same settings as in Section 4.2, and run FedConceptEM. By setting the number of models to $K = 4$ (large than the concept number 3), we show the distribution of $\gamma_{i,j;k}$ for FedConceptEM in Figure 8. The results indicate that data with concept shifts are assigned to models θ_1 , θ_3 , and θ_4 ; while data without concept shifts are not assigned to different models, resulting in little data assigned to θ_2 . Therefore, model θ_2 could be removed.

8.2 Adaptive ConceptEM

Our analysis in Section 8.1 illustrates the fact that when (1) the weights $\gamma_{i,j;k}$ converge in Algorithm 1 and (2) the number of models is larger than the number of concepts, we can decide the number of concepts by removing the model θ_k where $\sum_{i,j} \gamma_{i,j;k} \rightarrow 0$. The adaptive process is defined by first setting a large number of models K , and then checking if any model θ_k satisfies the following condition when the weights converge: $\frac{1}{N} \sum_{i=1}^M \sum_{j=1}^{N_i} \gamma_{i,j;k} < \delta$. The value of δ determines the threshold for removing a model. Once this condition is satisfied, we can remove the model k . For more details on removing the model, please see Appendix D.2.

⁵We exclude methods that cannot adapt to partial client participation.

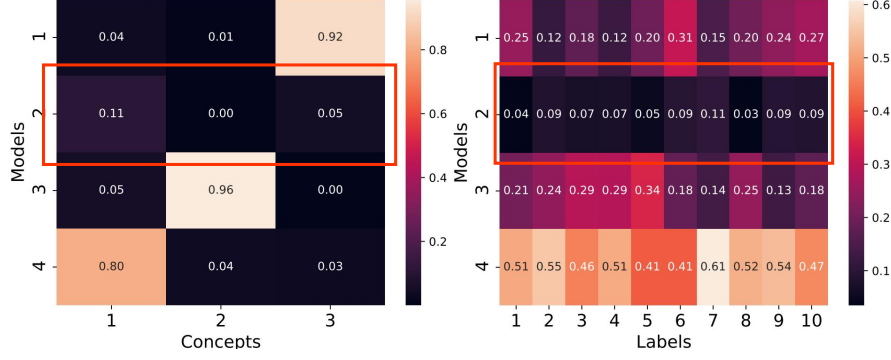


Figure 8: **Clustering results of FedConceptEM with $K = 4$.** We examine the distribution of $\gamma_{i,j;k}$ using the CIFAR10 dataset to illustrate the results of clustering (details refer to Section 7.1), under 3 concepts with 4 models. The figures in the red box demonstrate minimal weight assignment to model θ_2 .

Accelerating the convergence of $\gamma_{i,j;k}$ by Adam. The adaptive process presented above requires a full convergence of $\gamma_{i,j;k}$ before removing models, raising the necessity of speeding up the convergence of $\gamma_{i,j;k}$. A straightforward solution could be incorporating Adam (Kingma & Ba, 2014) into the optimization of $\gamma_{i,j,k}$, by assuming $\gamma_{i,j;k}^{t+1} - \gamma_{i,j;k}^t$ as the gradient of $\gamma_{i,j;k}$ on round t . Please refer to Appendix D.1 for an improved E-step. We show in Figure 10 and Figure 7 that FedConceptEM illustrates a faster convergence after introducing Adam.

Effectiveness of FedConceptEM in determining the optimal number of models. In Figure 7, we show 1) FedConceptEM can correctly find the number of concepts; 2) weights γ_{ijk} in FedConceptEM-Adam converge significantly faster than FedConceptEM (from 75 to 40 communication rounds); 3) FedEM failed to decide the number of concepts, and the performance is significantly worse than FedConceptEM.

9 Conclusion and Future Work

We propose FedConceptEM, a novel algorithm that addresses various distribution shifts in FL, including label, feature, and concept shifts. FedConceptEM has the potential to provide a better global initialization for personalized FL, provide first-level clustering in hierarchical clustering, and defend against backdoor attacks. Additionally, FedConceptEM can be expanded to adapt to changing circumstances by incorporating techniques from FedDrift (Jothimurugesan et al., 2022). This includes adding new models when a decrease in performance is detected and removing unnecessary models through the adaptive version of FedConceptEM.

References

- Briggs, C., Fan, Z., and Andras, P. Federated learning with hierarchical clustering of local updates to improve training on non-iid data. In *2020 International Joint Conference on Neural Networks (IJCNN)*, pp. 1–9. IEEE, 2020.
- Chen, X., Liu, S., Sun, R., and Hong, M. On the convergence of a class of adam-type algorithms for non-convex optimization. *arXiv preprint arXiv:1808.02941*, 2018.
- Deng, Y., Kamani, M. M., and Mahdavi, M. Adaptive personalized federated learning. *arXiv preprint arXiv:2003.13461*, 2020.
- Deng, Y., Kamani, M. M., and Mahdavi, M. Distributionally robust federated averaging, 2021.
- Fang, X. and Ye, M. Robust federated learning with noisy and heterogeneous clients. In *Proceedings of the IEEE/CVF Conference on Computer Vision and Pattern Recognition*, pp. 10072–10081, 2022.
- Gan, S., Mathur, A., Isopoussu, A., Kawsar, F., Berthouze, N., and Lane, N. Fruda: Framework for distributed adversarial domain adaptation. *IEEE Transactions on Parallel and Distributed Systems*, 2021.
- Ghosh, A., Chung, J., Yin, D., and Ramchandran, K. An efficient framework for clustered federated learning. *Advances in Neural Information Processing Systems*, 33:19586–19597, 2020.
- Guo, Y., Lin, T., and Tang, X. Towards federated learning on time-evolving heterogeneous data. *arXiv preprint arXiv:2112.13246*, 2021.
- He, K., Zhang, X., Ren, S., and Sun, J. Deep residual learning for image recognition. In *Proceedings of the IEEE conference on computer vision and pattern recognition*, pp. 770–778, 2016.
- Hendrycks, D. and Dietterich, T. Benchmarking neural network robustness to common corruptions and perturbations. *arXiv preprint arXiv:1903.12261*, 2019.
- Hsu, T.-M. H., Qi, H., and Brown, M. Measuring the effects of non-identical data distribution for federated visual classification. *arXiv preprint arXiv:1909.06335*, 2019.
- Jiang, L. and Lin, T. Test-time robust personalization for federated learning. In *International Conference on Learning Representations*, 2023.
- Jothimurugesan, E., Hsieh, K., Wang, J., Joshi, G., and Gibbons, P. B. Federated learning under distributed concept drift. *arXiv preprint arXiv:2206.00799*, 2022.
- Kairouz, P., McMahan, H. B., Avent, B., Bellet, A., Bennis, M., Bhagoji, A. N., Bonawitz, K., Charles, Z., Cormode, G., Cummings, R., et al. Advances and open problems in federated learning. *Foundations and Trends® in Machine Learning*, 14(1–2):1–210, 2021.
- Karimireddy, S. P., Jaggi, M., Kale, S., Mohri, M., Reddi, S. J., Stich, S. U., and Suresh, A. T. Mime: Mimicking centralized stochastic algorithms in federated learning. *arXiv preprint arXiv:2008.03606*, 2020a.
- Karimireddy, S. P., Kale, S., Mohri, M., Reddi, S., Stich, S., and Suresh, A. T. Scaffold: Stochastic controlled averaging for federated learning. In *International Conference on Machine Learning*, pp. 5132–5143. PMLR, 2020b.
- Ke, S., Huang, C., and Liu, X. Quantifying the impact of label noise on federated learning. *arXiv preprint arXiv:2211.07816*, 2022.
- Kingma, D. P. and Ba, J. Adam: A method for stochastic optimization. *arXiv preprint arXiv:1412.6980*, 2014.
- Li, H., Pan, S. J., Wang, S., and Kot, A. C. Domain generalization with adversarial feature learning. In *Proceedings of the IEEE conference on computer vision and pattern recognition*, pp. 5400–5409, 2018a.
- Li, Q., He, B., and Song, D. Model-contrastive federated learning. In *Proceedings of the IEEE/CVF Conference on Computer Vision and Pattern Recognition*, 2021.
- Li, T., Sahu, A. K., Zaheer, M., Sanjabi, M., Talwalkar, A., and Smith, V. Federated optimization in heterogeneous networks. *arXiv preprint arXiv:1812.06127*, 2018b.
- Li, T., Sahu, A. K., Zaheer, M., Sanjabi, M., Talwalkar, A., and Smith, V. Federated optimization in heterogeneous networks, 2018c. URL <https://arxiv.org/abs/1812.06127>.
- Lin, T., Stich, S. U., Patel, K. K., and Jaggi, M. Don’t use large mini-batches, use local sgd. In *International Conference on Learning Representations*, 2020. URL <https://openreview.net/forum?id=Bley01BFPr>.
- Marfoq, O., Neglia, G., Bellet, A., Kameni, L., and Vidal, R. Federated multi-task learning under a mixture of distributions. *Advances in Neural Information Processing Systems*, 34:15434–15447, 2021.
- McMahan, H. B., Moore, E., Ramage, D., Hampson, S., and Arcas, B. A. y. Communication-efficient learning of deep networks from decentralized data. 2016.

- Mertikopoulos, P., Hallak, N., Kavis, A., and Cevher, V. On the almost sure convergence of stochastic gradient descent in non-convex problems. *Advances in Neural Information Processing Systems*, 33:1117–1128, 2020.
- Mohri, M., Sivek, G., and Suresh, A. T. Agnostic federated learning, 2019.
- Muandet, K., Balduzzi, D., and Schölkopf, B. Domain generalization via invariant feature representation. In *International Conference on Machine Learning*, pp. 10–18. PMLR, 2013.
- Nguyen, T., Chen, G., and Chacon, L. An adaptive em accelerator for unsupervised learning of gaussian mixture models. *arXiv preprint arXiv:2009.12703*, 2020.
- Peng, X., Huang, Z., Zhu, Y., and Saenko, K. Federated adversarial domain adaptation, 2019. URL <https://arxiv.org/abs/1911.02054>.
- Reddi, S. J., Charles, Z., Zaheer, M., Garrett, Z., Rush, K., Konečný, J., Kumar, S., and McMahan, H. B. Adaptive federated optimization. In *International Conference on Learning Representations*, 2021. URL <https://openreview.net/forum?id=LkFG3lB13U5>.
- Reisizadeh, A., Farnia, F., Pedarsani, R., and Jadbabaie, A. Robust federated learning: The case of affine distribution shifts, 2020.
- Ruan, Y. and Joe-Wong, C. Fedsoft: Soft clustered federated learning with proximal local updating. In *Proceedings of the AAAI Conference on Artificial Intelligence*, volume 36, pp. 8124–8131, 2022.
- Sandler, M., Howard, A., Zhu, M., Zhmoginov, A., and Chen, L.-C. Mobilenetv2: Inverted residuals and linear bottlenecks. In *Proceedings of the IEEE conference on computer vision and pattern recognition*, pp. 4510–4520, 2018.
- Sattler, F., Müller, K.-R., and Samek, W. Clustered federated learning: Model-agnostic distributed multitask optimization under privacy constraints. *IEEE transactions on neural networks and learning systems*, 32(8):3710–3722, 2020a.
- Sattler, F., Müller, K.-R., Wiegand, T., and Samek, W. On the byzantine robustness of clustered federated learning. In *ICASSP 2020-2020 IEEE International Conference on Acoustics, Speech and Signal Processing (ICASSP)*, pp. 8861–8865. IEEE, 2020b.
- Shen, Y., Du, J., Zhao, H., Zhang, B., Ji, Z., and Gao, M. Fedmm: Saddle point optimization for federated adversarial domain adaptation. *arXiv preprint arXiv:2110.08477*, 2021.
- Stallmann, M. and Wilbik, A. Towards federated clustering: A federated fuzzy *c*-means algorithm (ffcm). *arXiv preprint arXiv:2201.07316*, 2022.
- Sun, Y., Chong, N., and Hideya, O. Multi-source domain adaptation based on federated knowledge alignment. *arXiv preprint arXiv:2203.11635*, 2022.
- T Dinh, C., Tran, N., and Nguyen, J. Personalized federated learning with moreau envelopes. *Advances in Neural Information Processing Systems*, 33:21394–21405, 2020.
- Wang, B., Li, G., Wu, C., Zhang, W., Zhou, J., and Wei, Y. A framework for self-supervised federated domain adaptation. *EURASIP Journal on Wireless Communications and Networking*, 2022(1):1–17, 2022a.
- Wang, H., Yurochkin, M., Sun, Y., Papailiopoulos, D., and Khazaeni, Y. Federated learning with matched averaging. *arXiv preprint arXiv:2002.06440*, 2020a.
- Wang, J., Liu, Q., Liang, H., Joshi, G., and Poor, H. V. Tackling the objective inconsistency problem in heterogeneous federated optimization. *arXiv preprint arXiv:2007.07481*, 2020b.
- Wang, J., Lan, C., Liu, C., Ouyang, Y., Qin, T., Lu, W., Chen, Y., Zeng, W., and Yu, P. Generalizing to unseen domains: A survey on domain generalization. *IEEE Transactions on Knowledge and Data Engineering*, 2022b.
- Wang, Z., Xu, H., Liu, J., Xu, Y., Huang, H., and Zhao, Y. Accelerating federated learning with cluster construction and hierarchical aggregation. *IEEE Transactions on Mobile Computing*, 2022c.
- Weiss, M. and Tonella, P. Simple techniques work surprisingly well for neural network test prioritization and active learning. In *Proceedings of the 31th ACM SIGSOFT International Symposium on Software Testing and Analysis*, 2022.
- Xie, M., Long, G., Shen, T., Zhou, T., Wang, X., Jiang, J., and Zhang, C. Multi-center federated learning. *arXiv preprint arXiv:2005.01026*, 2020.
- Xu, J., Chen, Z., Quek, T. Q., and Chong, K. F. E. Fedcorr: Multi-stage federated learning for label noise correction. In *Proceedings of the IEEE/CVF Conference on Computer Vision and Pattern Recognition*, pp. 10184–10193, 2022.
- Yurochkin, M., Agarwal, M., Ghosh, S., Greenewald, K., Hoang, N., and Khazaeni, Y. Bayesian nonparametric federated learning of neural networks. In *International Conference on Machine Learning*, pp. 7252–7261. PMLR, 2019.

Zhao, F., Huang, Y., Sai, A. M. V. V., and Wu, Y. A cluster-based solution to achieve fairness in federated learning. In *2020 IEEE Intl Conf on Parallel & Distributed Processing with Applications, Big Data & Cloud Computing, Sustainable Computing & Communications, Social Computing & Networking (ISPA/BDCLOUD/SocialCom/SustainCom)*, pp. 875–882. IEEE, 2020.

Contents of Appendix

A Proof of EM steps	16
B Proof of Theorem 5.2	17
C Related Works	22
D Experiment Details	23
D.1 E Steps of FedConceptEM-Adam	23
D.2 Removing the Models in Adaptive Process	23
D.3 Framework and Baseline Algorithms	23
D.4 Models and Hyper-parameter Settings	24
D.5 Datasets Construction	24
E Additional Experiment Results	24
E.1 Ablation Study on FedConceptEM	25
E.2 Ablation Study on Adaptive FedConceptEM	25

A Proof of EM steps

Theorem A.1. *Using EM algorithm to maximize Equation 8, the E-M steps are given by,*
E-step:

$$\gamma_{i,j;k}^t = \frac{\omega_{i;k}^{t-1} \tilde{\mathcal{L}}_k(\mathbf{x}_{ij}, y_{ij}, \boldsymbol{\theta}_k)}{\sum_{i=1}^K \omega_i^{t-1} \tilde{\mathcal{L}}_k(\mathbf{x}_{ij}, y_{ij}, \boldsymbol{\theta}_k)}. \quad (17)$$

M-step:

$$\omega_{i;k}^t = \frac{1}{N_i} \sum_{j=1}^{N_i} \gamma_{i,j;k}^t, \quad (18)$$

$$\boldsymbol{\theta}_k^t = \boldsymbol{\theta}_k^{t-1} - \frac{\eta}{N} \sum_{i=1}^M \sum_{j=1}^{N_i} \gamma_{i,j;k}^t \nabla_{\boldsymbol{\theta}_k^{t-1}} f_{ik}(\mathbf{x}_{ij}, y_{ij}, \boldsymbol{\theta}_k^{t-1}), \quad (19)$$

Proof. Consider the objective function,

$$\mathcal{L}(\boldsymbol{\Theta}, \boldsymbol{\Omega}) = \frac{1}{N} \sum_{i=1}^M \sum_{j=1}^{N_i} \ln \left(\sum_{k=1}^K \omega_{i;k} \tilde{\mathcal{L}}_k(\mathbf{x}_{ij}, y_{ij}; \boldsymbol{\theta}_k) \right) + \sum_{i=1}^M \lambda_i \left(\sum_{k=1}^K \omega_{i;k} - 1 \right), \quad (20)$$

Taking the derivative of $\mathcal{L}(\boldsymbol{\Theta})$, we have,

$$\frac{\partial \mathcal{L}(\boldsymbol{\Theta}, \boldsymbol{\Omega})}{\partial \omega_{i;k}} = \frac{1}{N} \sum_{i=1}^M \sum_{j=1}^{N_i} \frac{\tilde{\mathcal{L}}_k(\mathbf{x}_{ij}, y_{ij}; \boldsymbol{\theta}_k)}{\sum_{n=1}^K \omega_{i;n} \tilde{\mathcal{L}}_n(\mathbf{x}_{ij}, y_{ij}; \boldsymbol{\theta}_n)} + \sum_{i=1}^M \lambda_i, \quad (21)$$

setting $\lambda_i = -\frac{1}{N}$, and define

$$\gamma_{i,j;k} = \frac{\omega_{i;k} \tilde{\mathcal{L}}_k(\mathbf{x}_{ij}, y_{ij}; \boldsymbol{\theta}_k)}{\sum_{n=1}^K \omega_{i;n} \tilde{\mathcal{L}}_n(\mathbf{x}_{ij}, y_{ij}; \boldsymbol{\theta}_n)}, \quad (22)$$

and set $\frac{\partial \mathcal{L}(\boldsymbol{\Theta})}{\partial \omega_{i;k}} = 0$ to obtain the optimal $\omega_{i;k}$, we have,

$$\frac{1}{N} \sum_{i=1}^M \sum_{j=1}^{N_i} \frac{\gamma_{i,j;k}}{\omega_{i;k}} = \frac{1}{N} \sum_{i=1}^M N_i, \quad (23)$$

$$\omega_{i;k} = \frac{1}{N_i} \sum_{j=1}^{N_i} \gamma_{i,j;k}. \quad (24)$$

Then consider to optimize θ_k , we have,

$$\frac{\partial \mathcal{L}(\Theta, \Omega)}{\partial \theta_k} = \frac{1}{N} \sum_{i=1}^M \sum_{j=1}^{N_i} \frac{\omega_{i;k}}{\sum_{n=1}^K \omega_{i;n} \tilde{\mathcal{I}}_n(\mathbf{x}_{ij}, y_{ij}; \theta_n)} \cdot \frac{\partial \tilde{\mathcal{I}}_k(\mathbf{x}_{ij}, y_{ij}; \theta_k)}{\partial \theta_k}, \quad (25)$$

$$= \frac{1}{N} \sum_{i=1}^M \sum_{j=1}^{N_i} \frac{\omega_{i;k}}{\sum_{n=1}^K \omega_{i;n} \tilde{\mathcal{I}}_n(\mathbf{x}_{ij}, y_{ij}; \theta_n)} \cdot \frac{\exp(-f_{ik}(\mathbf{x}_{ij}, y_{ij}, \theta_k)) \sum_{i=1}^M \sum_{j=1}^N \gamma_{i,j;k}}{\sum_{i=1}^M \sum_{j=1}^N \mathbf{1}_{y_{ij}=y} \gamma_{i,j;k}} \cdot (-\nabla_{\theta_k} f_{ik}(\mathbf{x}_{ij}, y_{ij}, \theta_k)), \quad (26)$$

$$= -\frac{1}{N} \sum_{i=1}^M \sum_{j=1}^{N_i} \gamma_{i,j;k} \nabla_{\theta_k} f_{ik}(\mathbf{x}_{ij}, y_{ij}, \theta_k). \quad (27)$$

Because if hard to find a close-form solution to $\frac{\partial \mathcal{L}(\Theta, \Omega)}{\partial \theta_k} = 0$ when θ_k is the parameter of deep neural networks, we use gradient ascent to optimize θ_k . Then we finish the proof of E-M steps. \square

B Proof of Theorem 5.2

Lemma B.1. Define

$$h(\theta_x) = \frac{\omega_{i;k} \tilde{\mathcal{I}}_k(\mathbf{x}_{ij}, y_{ij}, \theta_x)}{\sum_{n=1}^K \omega_{i;n} \tilde{\mathcal{I}}_k(\mathbf{x}_{ij}, y_{ij}, \theta_n)}, \quad (28)$$

which corresponding to $\Theta = [\theta_1, \dots, \theta_x, \theta_{x+1}, \dots, \theta_K]$, we have,

$$|h(\theta_x) - h(\theta_y)| \leq \frac{L}{8} \|\theta_1 - \theta_2\|^2 + \frac{3}{8} \|\nabla f_{ik}(\mathbf{x}_{ij}, y_{ij}, \theta_y)\| \|\theta_1 - \theta_2\|. \quad (29)$$

Proof. Define,

$$h(\theta_x) = \frac{\omega_{i;k} \tilde{\mathcal{I}}_k(\mathbf{x}_{ij}, y_{ij}, \theta_x)}{\sum_{n=1}^K \omega_{i;n} \tilde{\mathcal{I}}_k(\mathbf{x}_{ij}, y_{ij}, \theta_n)}, \quad (30)$$

$$= \frac{\tilde{\omega}_{i;k} \exp(-f_{ik}(\mathbf{x}_{ij}, y_{ij}, \theta_x))}{\sum_{n=1}^K \tilde{\omega}_{i;n} \exp(-f_{ik}(\mathbf{x}_{ij}, y_{ij}, \theta_n))}, \quad (31)$$

where $\tilde{\omega}_{i;k} = \frac{\omega_{i;k}}{\mathcal{P}_k(y=y_{ij}; \theta_k)}$. Then we have,

$$\frac{\partial h(\theta_x)}{\partial \theta_x} = \frac{-\tilde{\omega}_{i;k} \exp(-f_{ik}(\mathbf{x}_{ij}, y_{ij}, \theta_x)) \nabla f_{ik}(\mathbf{x}_{ij}, y_{ij}, \theta_x)}{\sum_{n=1}^K \tilde{\omega}_{i;n} \exp(-f_{ik}(\mathbf{x}_{ij}, y_{ij}, \theta_n))} - \frac{-\tilde{\omega}_{i;k}^2 \exp^2(-f_{ik}(\mathbf{x}_{ij}, y_{ij}, \theta_x)) \nabla f_{ik}(\mathbf{x}_{ij}, y_{ij}, \theta_x)}{\left(\sum_{n=1}^K \tilde{\omega}_{i;n} \exp(-f_{ik}(\mathbf{x}_{ij}, y_{ij}, \theta_n))\right)^2}, \quad (32)$$

$$= \nabla f_{ik}(\mathbf{x}_{ij}, y_{ij}, \theta_x) h(\theta_x) (-1 + h(\theta_x)). \quad (33)$$

Then we have,

$$\|\nabla h(\theta_x) - \nabla h(\theta_y)\| = \|h(\theta_x) (1 - h(\theta_x)) \nabla f_{ik}(\mathbf{x}_{ij}, y_{ij}, \theta_x) - h(\theta_y) (1 - h(\theta_y)) \nabla f_{ik}(\mathbf{x}_{ij}, y_{ij}, \theta_y)\|, \quad (34)$$

$$\leq \frac{L}{4} \|\theta_x - \theta_y\| + \frac{1}{4} \|\nabla f_{ik}(\mathbf{x}_{ij}, y_{ij}, \theta_y)\|. \quad (35)$$

On the other hand, for $h(\theta_x)$, we can always find that,

$$h(\theta_x) = h(\theta_y) + \int_0^1 \langle \nabla h(\theta_y + \tau(\theta_x - \theta_y)), \theta_x - \theta_y \rangle d\tau, \quad (36)$$

$$= h(\theta_y) + \langle \nabla h(\theta_y), \theta_x - \theta_y \rangle + \int_0^1 \langle \nabla h(\theta_y + \tau(\theta_x - \theta_y)) - \nabla h(\theta_y), \theta_x - \theta_y \rangle d\tau. \quad (37)$$

Then we have,

$$|h(\boldsymbol{\theta}_x) - h(\boldsymbol{\theta}_y) - \langle \nabla h(\boldsymbol{\theta}_y), \boldsymbol{\theta}_x - \boldsymbol{\theta}_y \rangle| = \left| \int_0^1 \langle \nabla h(\boldsymbol{\theta}_y + \tau(\boldsymbol{\theta}_x - \boldsymbol{\theta}_y)) - \nabla h(\boldsymbol{\theta}_y), \boldsymbol{\theta}_x - \boldsymbol{\theta}_y \rangle d\tau \right|, \quad (38)$$

$$\leq \int_0^1 |\langle \nabla h(\boldsymbol{\theta}_y + \tau(\boldsymbol{\theta}_x - \boldsymbol{\theta}_y)) - \nabla h(\boldsymbol{\theta}_y), \boldsymbol{\theta}_x - \boldsymbol{\theta}_y \rangle| d\tau, \quad (39)$$

$$\leq \int_0^1 \|\nabla h(\boldsymbol{\theta}_y + \tau(\boldsymbol{\theta}_x - \boldsymbol{\theta}_y)) - \nabla h(\boldsymbol{\theta}_y)\| \|\boldsymbol{\theta}_x - \boldsymbol{\theta}_y\| d\tau, \quad (40)$$

$$\leq \int_0^1 \tau \left(\frac{L}{4} \|\boldsymbol{\theta}_x - \boldsymbol{\theta}_y\|^2 + \frac{1}{4} \|\nabla f_{ik}(\mathbf{x}_{ij}, y_{ij}, \boldsymbol{\theta}_y)\| \|\boldsymbol{\theta}_1 - \boldsymbol{\theta}_2\| \right) d\tau, \quad (41)$$

$$= \frac{L}{8} \|\boldsymbol{\theta}_x - \boldsymbol{\theta}_y\|^2 + \frac{1}{8} \|\nabla f_{ik}(\mathbf{x}_{ij}, y_{ij}, \boldsymbol{\theta}_y)\| \|\boldsymbol{\theta}_x - \boldsymbol{\theta}_y\|. \quad (42)$$

Therefore, we have,

$$|h(\boldsymbol{\theta}_x) - h(\boldsymbol{\theta}_y)| \leq \frac{L}{8} \|\boldsymbol{\theta}_1 - \boldsymbol{\theta}_2\|^2 + \frac{3}{8} \|\nabla f_{ik}(\mathbf{x}_{ij}, y_{ij}, \boldsymbol{\theta}_y)\| \|\boldsymbol{\theta}_x - \boldsymbol{\theta}_y\|. \quad (43)$$

□

Lemma B.2. Assume $g(x, y, \boldsymbol{\theta})$ is L -smooth (Assumption 1), define,

$$f(\boldsymbol{\theta}_k) = \frac{1}{N} \sum_{i=1}^M \sum_{j=1}^{N_i} \ln \left(\sum_{n=1}^K \omega_{i;n} \tilde{T}_n(\mathbf{x}_{ij}, y_{ij}; \boldsymbol{\theta}_n) \right), \quad (44)$$

where $1 \leq k \leq K$. Then we have,

$$\begin{aligned} & \|\nabla f(\boldsymbol{\theta}_1) - \nabla f(\boldsymbol{\theta}_2)\| \\ & \leq L \|\boldsymbol{\theta}_1 - \boldsymbol{\theta}_2\| + \frac{1}{N} \sum_{i=1}^M \sum_{j=1}^{N_i} \left(\frac{L}{8} \|\boldsymbol{\theta}_1 - \boldsymbol{\theta}_2\|^2 \|\nabla f_{ik}(\mathbf{x}_{ij}, y_{ij}, \boldsymbol{\theta}_2)\| + \frac{3}{8} \|\boldsymbol{\theta}_1 - \boldsymbol{\theta}_2\| \|\nabla f_{ik}(\mathbf{x}_{ij}, y_{ij}, \boldsymbol{\theta}_2)\|^2 \right), \end{aligned} \quad (45)$$

where $\gamma_{i,j;k}^1$ and $\gamma_{i,j;k}^2$ are defined in Theorem A.1 corresponding to $\boldsymbol{\Theta}_1$ and $\boldsymbol{\Theta}_2$ respectively. We can further prove that,

$$\begin{aligned} f(\boldsymbol{\theta}_1) & \leq f(\boldsymbol{\theta}_2) + \langle \nabla f(\boldsymbol{\theta}_2), \boldsymbol{\theta}_1 - \boldsymbol{\theta}_2 \rangle \\ & + \left(\frac{L}{2} + \frac{3}{16N} \sum_{i=1}^M \sum_{j=1}^{N_i} \|\nabla f_{ik}(\mathbf{x}_{ij}, y_{ij}, \boldsymbol{\theta}_2)\|^2 \right) \|\boldsymbol{\theta}_1 - \boldsymbol{\theta}_2\|^2 + \left(\frac{L}{16N} \sum_{i=1}^M \sum_{j=1}^{N_i} \|\nabla f_{ik}(\mathbf{x}_{ij}, y_{ij}, \boldsymbol{\theta}_2)\| \right) \|\boldsymbol{\theta}_1 - \boldsymbol{\theta}_2\|^3, \end{aligned} \quad (46)$$

$$\begin{aligned} f(\boldsymbol{\theta}_1) & \geq f(\boldsymbol{\theta}_2) + \langle \nabla f(\boldsymbol{\theta}_2), \boldsymbol{\theta}_1 - \boldsymbol{\theta}_2 \rangle \\ & - \left(\frac{L}{2} + \frac{3}{16N} \sum_{i=1}^M \sum_{j=1}^{N_i} \|\nabla f_{ik}(\mathbf{x}_{ij}, y_{ij}, \boldsymbol{\theta}_2)\|^2 \right) \|\boldsymbol{\theta}_1 - \boldsymbol{\theta}_2\|^2 - \left(\frac{L}{16N} \sum_{i=1}^M \sum_{j=1}^{N_i} \|\nabla f_{ik}(\mathbf{x}_{ij}, y_{ij}, \boldsymbol{\theta}_2)\| \right) \|\boldsymbol{\theta}_1 - \boldsymbol{\theta}_2\|^3. \end{aligned} \quad (47)$$

Proof. Based on the results in Theorem A.1, Section A, we have,

$$\frac{\partial f(\boldsymbol{\theta}_k)}{\partial \boldsymbol{\theta}_k} = -\frac{1}{N} \sum_{i=1}^M \sum_{j=1}^{N_i} \gamma_{i,j;k} \nabla_{\boldsymbol{\theta}_k} f_{ik}(\mathbf{x}_{ij}, y_{ij}, \boldsymbol{\theta}_k), \quad (48)$$

then we have,

$$\|\nabla f(\boldsymbol{\theta}_1) - \nabla f(\boldsymbol{\theta}_2)\| = \left\| \frac{1}{N} \sum_{i=1}^M \sum_{j=1}^{N_i} \gamma_{i,j;k}^1 \nabla f_{ik}(\mathbf{x}_{ij}, y_{ij}, \boldsymbol{\theta}_2) - \frac{1}{N} \sum_{i=1}^M \sum_{j=1}^{N_i} \gamma_{i,j;k}^2 \nabla f_{ik}(\mathbf{x}_{ij}, y_{ij}, \boldsymbol{\theta}_1) \right\|, \quad (49)$$

$$\leq \frac{1}{N} \sum_{i=1}^M \sum_{j=1}^{N_i} \left\| \gamma_{i,j;k}^1 \nabla f_{ik}(\mathbf{x}_{ij}, y_{ij}, \boldsymbol{\theta}_2) - \gamma_{i,j;k}^2 \nabla f_{ik}(\mathbf{x}_{ij}, y_{ij}, \boldsymbol{\theta}_1) \right\|, \quad (50)$$

$$\begin{aligned} &\leq \frac{1}{N} \sum_{i=1}^M \sum_{j=1}^{N_i} \gamma_{i,j;k}^1 \|\nabla f_{ik}(\mathbf{x}_{ij}, y_{ij}, \boldsymbol{\theta}_2) - \nabla f_{ik}(\mathbf{x}_{ij}, y_{ij}, \boldsymbol{\theta}_1)\| \\ &+ \frac{1}{N} \sum_{i=1}^M \sum_{j=1}^{N_i} |\gamma_{i,j;k}^1 - \gamma_{i,j;k}^2| \|\nabla f_{ik}(\mathbf{x}_{ij}, y_{ij}, \boldsymbol{\theta}_2)\|, \end{aligned} \quad (51)$$

$$\begin{aligned} &\leq L \|\boldsymbol{\theta}_1 - \boldsymbol{\theta}_2\| \\ &+ \frac{1}{N} \sum_{i=1}^M \sum_{j=1}^{N_i} \left(\frac{L}{8} \|\boldsymbol{\theta}_1 - \boldsymbol{\theta}_2\|^2 \|\nabla f_{ik}(\mathbf{x}_{ij}, y_{ij}, \boldsymbol{\theta}_2)\| + \frac{3}{8} \|\boldsymbol{\theta}_1 - \boldsymbol{\theta}_2\| \|\nabla f_{ik}(\mathbf{x}_{ij}, y_{ij}, \boldsymbol{\theta}_2)\|^2 \right). \end{aligned} \quad (52)$$

On the other hand, for $f(\boldsymbol{\theta}_k)$, we can always find that,

$$f(\boldsymbol{\theta}_1) = f(\boldsymbol{\theta}_2) + \int_0^1 \langle \nabla f(\boldsymbol{\theta}_2 + \tau(\boldsymbol{\theta}_1 - \boldsymbol{\theta}_2)), \boldsymbol{\theta}_1 - \boldsymbol{\theta}_2 \rangle d\tau, \quad (53)$$

$$= f(\boldsymbol{\theta}_2) + \langle \nabla f(\boldsymbol{\theta}_2), \boldsymbol{\theta}_1 - \boldsymbol{\theta}_2 \rangle + \int_0^1 \langle \nabla f(\boldsymbol{\theta}_2 + \tau(\boldsymbol{\theta}_1 - \boldsymbol{\theta}_2)) - \nabla f(\boldsymbol{\theta}_2), \boldsymbol{\theta}_1 - \boldsymbol{\theta}_2 \rangle d\tau. \quad (54)$$

Then we have,

$$\begin{aligned} &|f(\boldsymbol{\theta}_1) - f(\boldsymbol{\theta}_2) - \langle \nabla f(\boldsymbol{\theta}_2), \boldsymbol{\theta}_1 - \boldsymbol{\theta}_2 \rangle| \\ &= \left| \int_0^1 \langle \nabla f(\boldsymbol{\theta}_2 + \tau(\boldsymbol{\theta}_1 - \boldsymbol{\theta}_2)) - \nabla f(\boldsymbol{\theta}_2), \boldsymbol{\theta}_1 - \boldsymbol{\theta}_2 \rangle d\tau \right|, \end{aligned} \quad (55)$$

$$\leq \int_0^1 |\langle \nabla f(\boldsymbol{\theta}_2 + \tau(\boldsymbol{\theta}_1 - \boldsymbol{\theta}_2)) - \nabla f(\boldsymbol{\theta}_2), \boldsymbol{\theta}_1 - \boldsymbol{\theta}_2 \rangle| d\tau, \quad (56)$$

$$\leq \int_0^1 \|\nabla f(\boldsymbol{\theta}_2 + \tau(\boldsymbol{\theta}_1 - \boldsymbol{\theta}_2)) - \nabla f(\boldsymbol{\theta}_2)\| \|\boldsymbol{\theta}_1 - \boldsymbol{\theta}_2\| d\tau, \quad (57)$$

$$\begin{aligned} &\leq \int_0^1 \tau \left(\left(L + \frac{3}{8N} \sum_{i=1}^M \sum_{j=1}^{N_i} \|\nabla f_{ik}(\mathbf{x}_{ij}, y_{ij}, \boldsymbol{\theta}_2)\|^2 \right) \|\boldsymbol{\theta}_1 - \boldsymbol{\theta}_2\|^2 + \left(\frac{L}{8N} \sum_{i=1}^M \sum_{j=1}^{N_i} \|\nabla f_{ik}(\mathbf{x}_{ij}, y_{ij}, \boldsymbol{\theta}_2)\| \right) \|\boldsymbol{\theta}_1 - \boldsymbol{\theta}_2\|^3 \right) d\tau, \end{aligned} \quad (58)$$

$$\begin{aligned} &= \left(\frac{L}{2} + \frac{3}{16N} \sum_{i=1}^M \sum_{j=1}^{N_i} \|\nabla f_{ik}(\mathbf{x}_{ij}, y_{ij}, \boldsymbol{\theta}_2)\|^2 \right) \|\boldsymbol{\theta}_1 - \boldsymbol{\theta}_2\|^2 + \left(\frac{L}{16N} \sum_{i=1}^M \sum_{j=1}^{N_i} \|\nabla f_{ik}(\mathbf{x}_{ij}, y_{ij}, \boldsymbol{\theta}_2)\| \right) \|\boldsymbol{\theta}_1 - \boldsymbol{\theta}_2\|^3. \end{aligned} \quad (59)$$

Then we have,

$$f(\boldsymbol{\theta}_1) \leq f(\boldsymbol{\theta}_2) + \langle \nabla f(\boldsymbol{\theta}_2), \boldsymbol{\theta}_1 - \boldsymbol{\theta}_2 \rangle + \left(\frac{L}{2} + \frac{3}{16N} \sum_{i=1}^M \sum_{j=1}^{N_i} \|\nabla f_{ik}(\mathbf{x}_{ij}, y_{ij}, \boldsymbol{\theta}_2)\|^2 \right) \|\boldsymbol{\theta}_1 - \boldsymbol{\theta}_2\|^2 + \left(\frac{L}{16N} \sum_{i=1}^M \sum_{j=1}^{N_i} \|\nabla f_{ik}(\mathbf{x}_{ij}, y_{ij}, \boldsymbol{\theta}_2)\| \right) \|\boldsymbol{\theta}_1 - \boldsymbol{\theta}_2\|^3, \quad (60)$$

$$f(\boldsymbol{\theta}_1) \geq f(\boldsymbol{\theta}_2) + \langle \nabla f(\boldsymbol{\theta}_2), \boldsymbol{\theta}_1 - \boldsymbol{\theta}_2 \rangle - \left(\frac{L}{2} + \frac{3}{16N} \sum_{i=1}^M \sum_{j=1}^{N_i} \|\nabla f_{ik}(\mathbf{x}_{ij}, y_{ij}, \boldsymbol{\theta}_2)\|^2 \right) \|\boldsymbol{\theta}_1 - \boldsymbol{\theta}_2\|^2 - \left(\frac{L}{16N} \sum_{i=1}^M \sum_{j=1}^{N_i} \|\nabla f_{ik}(\mathbf{x}_{ij}, y_{ij}, \boldsymbol{\theta}_2)\| \right) \|\boldsymbol{\theta}_1 - \boldsymbol{\theta}_2\|^3. \quad (61)$$

□

Theorem B.3 (Convergence rate of ConceptEM). *Assume f_{ik} is L -smooth (Assumption 1), setting T as the number of iterations, and $\eta = \frac{8}{27L+9\sigma^2}$, we have,*

$$\frac{1}{T} \sum_{t=0}^{T-1} \sum_{k=1}^K \|\nabla_{\boldsymbol{\theta}_k} \mathcal{L}(\boldsymbol{\Theta}^t)\|^2 \leq O\left(\frac{(27L+9\sigma^2)(\mathcal{L}(\boldsymbol{\Theta}^*) - \mathcal{L}(\boldsymbol{\Theta}^0))}{4T}\right), \quad (62)$$

which denotes the algorithm achieve sub-linear convergence rate.

Proof. Each M step of ConceptEM can be seen as optimizing $\boldsymbol{\theta}_1, \dots, \boldsymbol{\theta}_K$ respectively. Then we have,

$$\mathcal{L}(\boldsymbol{\Theta}^{t+1}) - \mathcal{L}(\boldsymbol{\Theta}^t) = \sum_{k=1}^K \mathcal{L}(\boldsymbol{\Theta}_k^t) - \mathcal{L}(\boldsymbol{\Theta}_{k-1}^t), \quad (63)$$

where we define,

$$\boldsymbol{\Theta}_k^t = [\boldsymbol{\theta}_1^{t+1}, \dots, \boldsymbol{\theta}_k^{t+1}, \boldsymbol{\theta}_{k+1}^t \dots, \boldsymbol{\theta}_K^t], \quad (64)$$

and $\boldsymbol{\Theta}_0^t = \boldsymbol{\Theta}^t$, $\boldsymbol{\Theta}_K^t = \boldsymbol{\Theta}^{t+1}$. Then we define,

$$f_k(\boldsymbol{\theta}_\nu) = \frac{1}{N} \sum_{i=1}^M \sum_{j=1}^{N_i} \ln \left(\sum_{n=1}^K \omega_{i;n} \tilde{\mathcal{I}}_{in}(\mathbf{x}_{ij}, y_{ij}; \boldsymbol{\theta}_n) \right), \quad (65)$$

where $\boldsymbol{\theta}_n \in \boldsymbol{\Theta}_k^t$ for $n \neq \nu$, and $\boldsymbol{\theta}_\nu$ is the variable in $f_k(\boldsymbol{\theta}_\nu)$. Define $\gamma_{i,j;k}^k$ that corresponding to $\boldsymbol{\Theta}_k$, we have,

$$\begin{aligned} & \mathcal{L}(\boldsymbol{\Theta}^{t+1}) - \mathcal{L}(\boldsymbol{\Theta}^t) \\ &= \sum_{k=1}^K \mathcal{L}(\boldsymbol{\Theta}_k^t) - \mathcal{L}(\boldsymbol{\Theta}_{k-1}^t), \end{aligned} \quad (66)$$

$$= \sum_{k=1}^K f_k(\boldsymbol{\theta}_k^{t+1}) - f_k(\boldsymbol{\theta}_k^t), \quad (67)$$

$$\begin{aligned} & \geq \sum_{k=1}^K \langle \nabla f_k(\boldsymbol{\theta}_k^t), \boldsymbol{\theta}_k^{t+1} - \boldsymbol{\theta}_k^t \rangle, \\ & - \left(\frac{L}{2} + \frac{3}{16N} \sum_{i=1}^M \sum_{j=1}^{N_i} \|\nabla f_{ik}(\mathbf{x}_{ij}, y_{ij}, \boldsymbol{\theta}_k^t)\|^2 \right) \|\boldsymbol{\theta}_k^{t+1} - \boldsymbol{\theta}_k^t\|^2 - \left(\frac{L}{16N} \sum_{i=1}^M \sum_{j=1}^{N_i} \|\nabla f_{ik}(\mathbf{x}_{ij}, y_{ij}, \boldsymbol{\theta}_k^t)\| \right) \|\boldsymbol{\theta}_k^{t+1} - \boldsymbol{\theta}_k^t\|^3. \end{aligned} \quad (68)$$

The last inequality comes from Lemma B.2. From the results in Theorem A.1, Section A, we have,

$$\nabla f_k(\boldsymbol{\theta}_k^t) = -\frac{1}{N} \sum_{i=1}^M \sum_{j=1}^{N_i} \gamma_{i,j;k}^k \nabla_{\boldsymbol{\theta}_k} f_{ik}(\mathbf{x}_{ij}, y_{ij}, \boldsymbol{\theta}_k), \quad (69)$$

at the same time, we have,

$$\boldsymbol{\theta}_k^{t+1} - \boldsymbol{\theta}_k^t = \eta \nabla f_0(\boldsymbol{\theta}_k) = -\frac{\eta}{N} \sum_{i=1}^M \sum_{j=1}^{N_i} \gamma_{i,j;k}^0 \nabla_{\boldsymbol{\theta}_k} f_{ik}(\mathbf{x}_{ij}, y_{ij}, \boldsymbol{\theta}_k). \quad (70)$$

Then we can obtain,

$$\begin{aligned} & \langle \nabla f_k(\boldsymbol{\theta}_k^t), \boldsymbol{\theta}_k^{t+1} - \boldsymbol{\theta}_k^t \rangle \\ &= \langle \nabla f_k(\boldsymbol{\theta}_k^t) - \nabla f_0(\boldsymbol{\theta}_k) + \nabla f_0(\boldsymbol{\theta}_k), \boldsymbol{\theta}_k^{t+1} - \boldsymbol{\theta}_k^t \rangle, \end{aligned} \quad (71)$$

$$= \langle \nabla f_k(\boldsymbol{\theta}_k^t) - \nabla f_0(\boldsymbol{\theta}_k), \boldsymbol{\theta}_k^{t+1} - \boldsymbol{\theta}_k^t \rangle + \langle \nabla f_0(\boldsymbol{\theta}_k), \boldsymbol{\theta}_k^{t+1} - \boldsymbol{\theta}_k^t \rangle, \quad (72)$$

$$\geq -\|\nabla f_k(\boldsymbol{\theta}_k^t) - \nabla f_0(\boldsymbol{\theta}_k)\| \|\boldsymbol{\theta}_k^{t+1} - \boldsymbol{\theta}_k^t\| + \frac{1}{\eta} \|\boldsymbol{\theta}_k^{t+1} - \boldsymbol{\theta}_k^t\|^2, \quad (73)$$

$$\geq \left(\frac{1}{\eta} - L - \frac{3}{8N} \sum_{i=1}^M \sum_{j=1}^{N_i} \|\nabla f_{ik}(\mathbf{x}_{ij}, y_{ij}, \boldsymbol{\theta}_k^t)\|^2 \right) \|\boldsymbol{\theta}_k^{t+1} - \boldsymbol{\theta}_k^t\|^2 - \left(\frac{L}{8N} \sum_{i=1}^M \sum_{j=1}^{N_i} \|\nabla f_{ik}(\mathbf{x}_{ij}, y_{ij}, \boldsymbol{\theta}_k^t)\| \right) \|\boldsymbol{\theta}_k^{t+1} - \boldsymbol{\theta}_k^t\|^3. \quad (74)$$

Combine Equation (68) and Equation (74), we have,

$$\begin{aligned} & \mathcal{L}(\boldsymbol{\Theta}^{t+1}) - \mathcal{L}(\boldsymbol{\Theta}^t) \\ & \geq \sum_{k=1}^K \left(\frac{1}{\eta} - \frac{3L}{2} - \frac{9}{16N} \sum_{i=1}^M \sum_{j=1}^{N_i} \|\nabla f_{ik}(\mathbf{x}_{ij}, y_{ij}, \boldsymbol{\theta}_k^t)\|^2 \right) \|\boldsymbol{\theta}_k^{t+1} - \boldsymbol{\theta}_k^t\|^2 \\ & \quad - \left(\frac{3L}{16N} \sum_{i=1}^M \sum_{j=1}^{N_i} \|\nabla f_{ik}(\mathbf{x}_{ij}, y_{ij}, \boldsymbol{\theta}_k^t)\| \right) \|\boldsymbol{\theta}_k^{t+1} - \boldsymbol{\theta}_k^t\|^3, \end{aligned} \quad (75)$$

$$\begin{aligned} & \geq \sum_{k=1}^K \left(\frac{1}{\eta} - \frac{3L}{2} - \frac{9\sigma^2}{16} \right) \|\boldsymbol{\theta}_k^{t+1} - \boldsymbol{\theta}_k^t\|^2 \\ & \quad - \frac{3L}{16N} \left(\sum_{i=1}^M \sum_{j=1}^{N_i} \|\nabla f_{ik}(\mathbf{x}_{ij}, y_{ij}, \boldsymbol{\theta}_k^t)\| \right) \left\| \frac{\eta}{N} \sum_{i=1}^M \sum_{j=1}^{N_i} \gamma_{i,j;k}^0 \nabla f_{ik}(\mathbf{x}_{ij}, y_{ij}, \boldsymbol{\theta}_k^t) \right\| \|\boldsymbol{\theta}_k^{t+1} - \boldsymbol{\theta}_k^t\|^2, \end{aligned} \quad (76)$$

$$\geq \sum_{k=1}^K \left(\frac{1}{\eta} - \frac{3L}{2} - \frac{9\sigma^2}{16} \right) \|\boldsymbol{\theta}_k^{t+1} - \boldsymbol{\theta}_k^t\|^2 - \frac{3\eta L}{16} \left(\frac{1}{N} \sum_{i=1}^M \sum_{j=1}^{N_i} \|\nabla f_{ik}(\mathbf{x}_{ij}, y_{ij}, \boldsymbol{\theta}_k^t)\| \right)^2 \|\boldsymbol{\theta}_k^{t+1} - \boldsymbol{\theta}_k^t\|^2, \quad (77)$$

$$\geq \sum_{k=1}^K \left(\frac{1}{\eta} - \frac{3L}{2} - \frac{9\sigma^2}{16} - \frac{3\eta L \sigma^2}{16} \right) \|\boldsymbol{\theta}_k^{t+1} - \boldsymbol{\theta}_k^t\|^2, \quad (78)$$

$$= \sum_{k=1}^K \left(\eta - \frac{3L\eta^2}{2} - \frac{9\sigma^2\eta^2}{16} - \frac{3\eta^3 L \sigma^2}{16} \right) \|\nabla_{\boldsymbol{\theta}_k} \mathcal{L}(\boldsymbol{\Theta}^t)\|^2. \quad (79)$$

Then we can observe that the objective $\mathcal{L}(\boldsymbol{\Theta})$ converge when,

$$\eta \leq \frac{((576L^2 + 624L\sigma^2 + 81\sigma^4)^{1/2} - 24L - 9\sigma^2)}{6L\sigma^2}, \quad (80)$$

and when we set,

$$\eta \leq \frac{((576L^2 + 528L\sigma^2 + 81\sigma^4)^{1/2} - 24L - 9\sigma^2)}{6L\sigma^2}, \quad (81)$$

$$= \frac{\sqrt{(24L + 9\sigma^2)^2 + 96L\sigma^2} - (24L + 9\sigma^2)}{6L\sigma^2}, \quad (82)$$

we have,

$$\mathcal{L}(\Theta^{t+1}) - \mathcal{L}(\Theta^t) \geq \frac{\eta}{2} \sum_{k=1}^K \|\nabla f_0(\theta_k^t)\|^2, \quad (83)$$

$$= \frac{\eta}{2} \sum_{k=1}^K \|\nabla_{\theta_k} \mathcal{L}(\Theta^t)\|^2. \quad (84)$$

Then we have,

$$\mathcal{L}(\Theta^T) - \mathcal{L}(\Theta^0) = \sum_{t=0}^{T-1} \mathcal{L}(\Theta^{t+1}) - \mathcal{L}(\Theta^t), \quad (85)$$

$$\geq \frac{\eta}{2} \sum_{t=0}^{T-1} \sum_{k=1}^K \|\nabla_{\theta_k} \mathcal{L}(\Theta^t)\|^2. \quad (86)$$

Because

$$\frac{1}{\eta} = \frac{6L\sigma^2}{\sqrt{(24L + 9\sigma^2)^2 + 96L\sigma^2} - (24L + 9\sigma^2)}, \quad (87)$$

$$= \frac{6L\sigma^2 \left(\sqrt{(24L + 9\sigma^2)^2 + 96L\sigma^2} + (24L + 9\sigma^2) \right)}{96L\sigma^2}, \quad (88)$$

$$= \frac{\sqrt{(24L + 9\sigma^2)^2 + 96L\sigma^2} + (24L + 9\sigma^2)}{16}, \quad (89)$$

$$\leq \frac{54L + 18\sigma^2}{16}, \quad (90)$$

$$= \frac{27L + 9\sigma^2}{8}. \quad (91)$$

That is,

$$\frac{1}{T} \sum_{t=0}^{T-1} \sum_{k=1}^K \|\nabla_{\theta_k} \mathcal{L}(\Theta^t)\|^2 \leq \frac{(27L + 9\sigma^2) (\mathcal{L}(\Theta^*) - \mathcal{L}(\Theta^0))}{4T}. \quad (92)$$

□

C Related Works

Federated Learning with label distribution shifts. As the de facto FL algorithm, McMahan et al. (2016); Lin et al. (2020) proposes to use local SGD steps to alleviate the communication bottleneck. However, the non-iid nature of local distribution hinders the performance of FL algorithms (Li et al., 2018c; Wang et al., 2020b; Karimireddy et al., 2020b,a; Guo et al., 2021; Jiang & Lin, 2023). Therefore, designing algorithms to deal with the distribution shifts over clients is a key problem in FL (Kairouz et al., 2021). Most existing works only consider the label distribution skew among clients. Some techniques address local distribution shifts by training robust global models (Li et al., 2018c, 2021), while others use variance reduction methods (Karimireddy et al., 2020b,a). However, the proposed methods cannot be used directly for concept shift because the decision boundary changes. Combining FedConceptEM with other methods that address label distribution shifts may be an interesting future direction, but it is orthogonal to our approach in this work.

Federated Learning with feature distribution shifts. Studies about feature distribution skew in FL mostly focus on domain generalization (DG) problem that aims to train robust models that can generalize to unseen feature distributions. Reisizadeh et al. (2020) investigates a special case that the local distribution is perturbed by an affine function, i.e. from x to $Ax + b$. Many studies focus on adapting DG algorithms for FL scenarios. For example, combining FL with Distribution Robust Optimization (DRO), resulting in robust models that perform well on all clients (Mohri et al., 2019; Deng et al., 2021); combining FL with techniques that learn domain invariant features (Peng et al., 2019; Wang et al., 2022a; Shen et al., 2021; Sun et al., 2022; Gan et al., 2021) to improve the generalization ability of trained models. All of the above methods aim to train a single robust feature extractor that can generalize well on unseen distributions. However, using a single model cannot solve the diverse distribution shift challenge, as the decision boundary changes when concept shifts occur.

Federated Learning with concept shifts. Concept shift is not a well-studied problem in FL. However, some special cases become an emerging topic recently. For example, research has shown that label noise can negatively impact model performance (Ke et al., 2022). Additionally, methods have been proposed to correct labels that have been corrupted by noise (Fang & Ye, 2022; Xu et al., 2022). Recently, Jothimurugesan et al. (2022) also investigate the concept shift problem under the assumption that clients do not have concept shifts at the beginning of the training. However, it is difficult to ensure the non-existence of concept shifts when information about local distributions is not available in practice. Additionally, Jothimurugesan et al. (2022) did not address the issue of label and feature distribution skew. In this work, we consider a more realistic but more challenging scenario where clients could have all three kinds of shifts with each other, unlike Jothimurugesan et al. (2022) that needs to restrict the non-occurrence of concept shift at the initial training phase.

Clustered Federated Learning. Clustered Federated Learning (clustered FL) is a technique that groups clients into clusters based on their local data distribution to address the distribution shift problem. Various methods have been proposed for clustering clients, including using local loss values (Ghosh et al., 2020), communication time/local calculation time (Wang et al., 2022c), fuzzy c -Means (Stallmann & Wilbik, 2022), and hierarchical clustering (Zhao et al., 2020; Briggs et al., 2020; Sattler et al., 2020a). Some approaches, such as FedSoft (Ruan & Joe-Wong, 2022), combine clustered FL with personalized FL by using a soft cluster mechanism that allows clients to contribute to multiple clusters. Other methods, such as FeSEM (Xie et al., 2020) and FedEM (Marfoq et al., 2021), employ an Expectation-Maximization (EM) approach and utilize the log-likelihood objective function, as in traditional EM. Our proposed FedConceptEM overcomes the pitfalls of FedEM, and shows strong empirical effectiveness over other clustered FL methods. It is noteworthy that FedConceptEM could further complement other clustered FL methods for larger performance gain.

D Experiment Details

D.1 E Steps of FedConceptEM-Adam

We summarize the E steps of FedConceptEM-Adam as follows:

$$\tilde{\gamma}_{i,j;k}^t = \frac{\omega_{i,k}^{t-1} \tilde{\mathcal{I}}_k(\mathbf{x}_{i,j}, y_{i,j}, \boldsymbol{\theta}_k)}{\sum_{n=1}^K \omega_{i,n}^{t-1} \tilde{\mathcal{I}}_k(\mathbf{x}_{i,j}, y_{i,j}, \boldsymbol{\theta}_k)}, \quad (93)$$

$$g_{i,j;k} = \gamma_{i,j;k}^{t-1} - \tilde{\gamma}_{i,j;k}^t, \quad (94)$$

$$\nu_{i,j;k}^t = (1 - \beta_1)g_{i,j;k} + \beta_1 \nu_{i,j;k}^{t-1}, \quad (95)$$

$$a_{i,j;k}^t = (1 - \beta_2)g_{i,j;k}^2 + \beta_2 a_{i,j;k}^{t-1}, \quad (96)$$

$$\gamma_{i,j;k}^t = \gamma_{i,j;k}^{t-1} - \alpha \frac{\nu_{i,j;k}^t / (1 - \beta_1)}{\sqrt{a_{i,j;k}^t / (1 - \beta_2) + \epsilon}}, \quad (97)$$

$$\gamma_{i,j;k}^t = \frac{\max(\gamma_{i,j;k}^t, 0)}{\sum_{n=1}^K \max(\gamma_{i,j;n}^t, 0)}, \quad (98)$$

where we set $\alpha = 1.0$, $\beta_1 = 0.9$, $\beta_2 = 0.99$, and $\epsilon = 1e - 8$ in practice by default. The Equation (98) is to avoid $\gamma_{i,j;k}^t < 0$ after adding the momentum.

D.2 Removing the Models in Adaptive Process

In Algorithm 2, we show how to remove the models once we decide the model could be removed. Once the model $\boldsymbol{\theta}_k$ is decided to be removed, the server will broadcast to all the clients, and clients will remove the local models, and normalize $\gamma_{i,j;k}$ and $\omega_{i,k}$ by Line 7 and Line 9 in Algorithm 2.

D.3 Framework and Baseline Algorithms

We extend the public code provided by Marfoq et al. (2021) in this work. For personalized algorithms that don't have a global model, we average the local models to create a global model and evaluate it on global test datasets. When testing non-participating clients on clustered FL algorithms (IFCA, CFL, and FeSEM), we assign them to the cluster they performed best on during training.

Algorithm 2 Check and remove model in FedConceptEM

Require: Threshold value δ , number of clients M , number of data in each client N_i , number of model K , $\gamma_k =$

```
 $\frac{1}{N} \sum_{i=1}^M \sum_{j=1}^{N_i} \gamma_{i,j;k}$  for each  $k$ .  
1: for model  $k = 1, \dots, K$  do  
2:   if  $\frac{1}{N} \sum_{i=1}^M \sum_{j=1}^{N_i} \gamma_{i,j;k} < \delta$  then  
3:     Remove model  $k$ .  
4:     for client  $i = 1, \dots, M$  do  
5:       Remove  $\gamma_{i,j;k}$  for all  $j$ .  
6:       for client  $\tau = 1, \dots, K, \tau \neq k$  do  
7:          $\gamma_{i,j;\tau} = \frac{\gamma_{i,j;\tau}}{\sum_{\tau'} \gamma_{i,j;\tau'}}$  for all  $j$ .  
8:       Remove  $\omega_{i,k}$ .  
9:       Update  $\omega_{i;\tau}$  by Equation (11) for all  $\tau \neq k$ .
```

D.4 Models and Hyper-parameter Settings

We use a three-layer CNN for the FashionMNIST dataset, and use pre-trained MobileNetV2 (Sandler et al., 2018) for CIFAR10 and CIFAR100 datasets. We set the batch size to 128, and run 1 local epoch in each communication round by default. We use SGD optimizer and set the momentum to 0.9. The learning rates are chosen in $[0.01, 0.03, 0.06, 0.1]$, and we run each algorithm for 200 communication rounds, and report the best result of each algorithm. We also include the results of CIFAR10 and CIFAR100 datasets using ResNet18 (He et al., 2016) in Table 2. For each clustered FL algorithm (including FedConceptEM), we initialize 3 models by default following the ideal case. We also investigate the adaptive process by initialize 6 models at the beginning in Figure 7.

D.5 Datasets Construction

FashionMNIST dataset. We split the FashionMNIST dataset into 300 groups of clients using LDA with a value of 1.0 for alpha. 30% of the clients will not have any changes to their images or labels. For 20% of the clients, labels will not be changed, and we will add synthetic corruptions following the idea of FashionMNIST-C with a random level of severity from 1 to 5. 25% of the clients will have their labels changed to $C - 1 - y$, where C is the number of classes, and y is the true label. We will also add synthetic corruption to 20% of these clients (5% of 300 clients). Finally, 25% of the clients will have their labels changed to $(y + 1) \bmod C$, and we will also add synthetic corruptions to 20% of these clients.

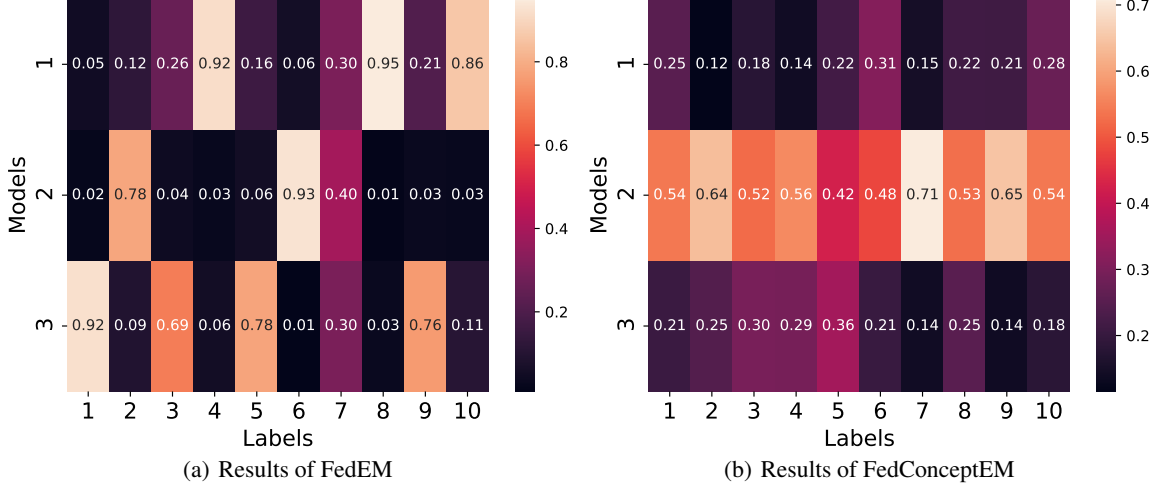
CIFAR10 and CIFAR100 datasets. For the MobileNetV2 model, we divided the dataset into 300 smaller groups of data (called "clients"). To ensure that each group had enough data to be well-trained, we first made three copies of the original dataset. Then, we used a technique called Latent Dirichlet Allocation (LDA) with a parameter of $\alpha = 1.0$ to divide the dataset into the 300 clients. For the ResNet18 model, we also used LDA with $\alpha = 1.0$, but we divided the dataset into 100 clients without making any copies. Then 30% of the clients will not have any changes to their images or labels. For 20% of the clients, labels will not be changed, and we will add synthetic corruptions following the idea of FashionMNIST-C with a random level of severity from 1 to 5. 25% of the clients will have their labels changed to $C - 1 - y$, where C is the number of classes, and y is the true label. We will also add synthetic corruption to 20% of these clients (5% of 300 clients). Finally, 25% of the clients will have their labels changed to $(y + 1) \bmod C$, and we will also add synthetic corruptions to 20% of these clients.

Test clients construction. We directly use the test datasets provided by FashionMNIST, CIFAR10, and CIFAR100 datasets, and construct 3 test clients. The labels for the first client remain unchanged. For the second client, the labels are changed to $C - 1 - y$, and for the third client, the labels are changed to $(y + 1) \bmod C$.

E Additional Experiment Results

The results of clustering the data using FedEM and FedConceptEM are illustrated in Figure 9. This figure shows the proportion of data that is assigned to each model, which can be seen as an approximation of $\mathcal{P}_k(y; \theta_k)$. The results indicate that: 1) The clustering of FedEM is primarily affected by label distribution shift, which leads to poor global accuracy, as demonstrated in Table 1. 2) In contrast, the label distribution within each model θ_k of FedConceptEM is relatively balanced, resulting in improved robustness of the trained models, as shown in Table 1.

Figure 9: **Clustering results of FedEM and FedConceptEM on label distribution.** In this figure, we investigate the distribution of $\gamma_{i,j;k}$ using the CIFAR10 dataset and construct clients with three concepts (refer to Section 7.1 for more details). Our aim is to examine how the FedEM and FedConceptEM algorithms divide clients into different models. For each grid (l, k) in the figures, we calculate the proportion of data of label l that assigns weights to θ_k . The data in grids with different concepts will have different labels. We find that the clustering results of FedEM is dominated by label distribution, and the label distribution within each model k of FedConceptEM is relatively balanced.



E.1 Ablation Study on FedConceptEM

In this section, we present additional findings from our ablation study on local steps, concept count, and client involvement.

Ablation studies on local steps. In Table 3, we demonstrate the impact of the number of local epochs on the performance of different algorithms. Our results indicate that FedConceptEM consistently outperforms the other baseline algorithms, even as the number of local epochs increases. However, we also observe that FedConceptEM is relatively sensitive to the number of local epochs. This may be due to the fact that a large number of local steps can cause the parameters to drift away from the true global optima, as previously reported in several FL studies (e.g. (Karimireddy et al., 2020b; Li et al., 2018b, 2021)). In the E step, this can make it more difficult for the algorithm to accurately find $\gamma_{i,j;k}$ based on sub-optimal parameters.

Ablation studies on partial client participation. We have included the ablation study about the number of clients participating in each round in the main paper. In Table 4, we report the final accuracies on both local and global test datasets to include more details. Results show FedConceptEM is robust to the partial client participation.

Ablation study on the number of concepts. We change the number of concepts in $[1, 3, 5]$, and report the local and global accuracy in Table 5. Results show that: 1) FedConceptEM always achieves the best global accuracy compare with other algorithms, indicating the robustness of trained models by FedConceptEM. 2) Although FedEM may achieve better local accuracy, the generalization ability of trained models is poor and we believe that it is an over-fitting to local data.

E.2 Ablation Study on Adaptive FedConceptEM

In this section, we present the ablation studies on value of δ and the convergence curve of FedConceptEM compare with FedConceptEM-Adam.

FedConceptEM-Adam converges significantly faster than FedConceptEM. Figure 10 shows that FedConceptEM-Adam converges faster than FedConceptEM at the initial training phase. Figure 7 also shows that FedConceptEM-Adam makes $\gamma_{i,j;k}$ converge faster.

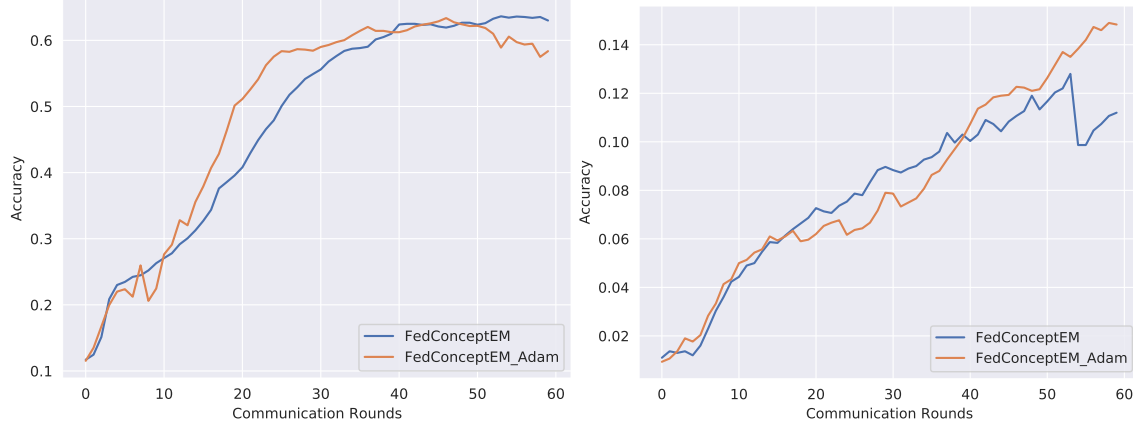


Figure 10: **Convergence speed up of ConceptEM-Adam.** We run ConceptEM and ConceptEM on CIFAR10 and CIFAR100 datasets with $K = 3$, and report the global accuracy on each communication rounds. We do not use the adaptive process here.

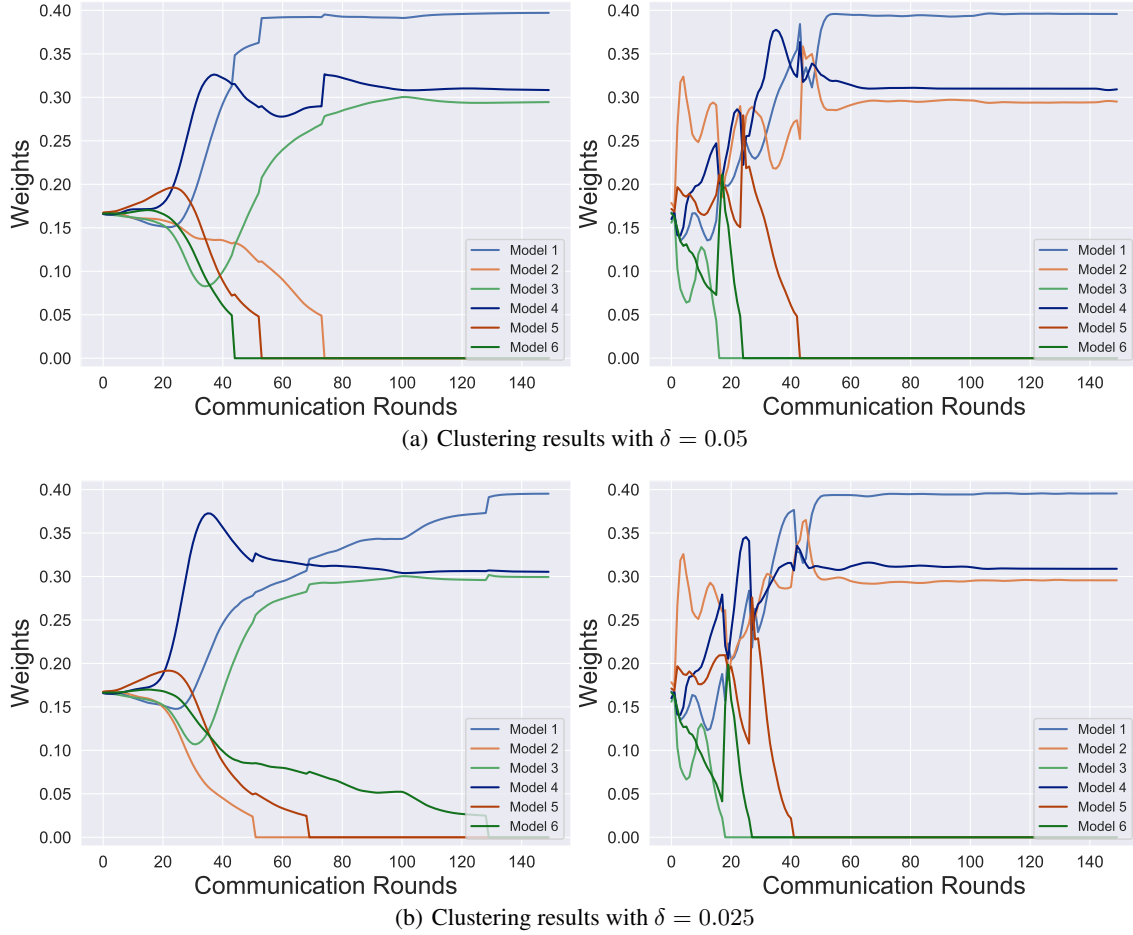


Figure 11: **Clustering results of FedConceptEM and FedConceptEM-Adam on different δ** We split CIFAR10 dataset to 300 clients, initialize 6 models, and report clustering results by calculating weights by $\sum_{i,j} \gamma_{i,j;k} / \sum_{i,j,k} \gamma_{i,j;k}$, which represents the portion of clients that choose the model k .

Table 3: **Ablation study on the number of local epochs.** We split CIFAR10 dataset into 300 clients, and set the number of local epochs to $\{1, 5\}$. We run algorithms for 200 communication rounds, and report the global accuracy on the round that achieves the best train accuracy.

Algorithm	1		5	
	Local	Global	Local	Global
FedAvg	30.28	30.47	29.75	29.60
IFCA	43.76	26.62	43.49	35.50
FeSEM	45.32	30.79	38.32	24.33
FedSoft	83.08	22.00	82.20	19.67
FedEM	51.31	43.35	55.69	50.17
FedConceptEM	62.74	63.83	57.31	57.43

Table 4: **Ablation study on the number of clients participating in each round.** We Split CIFAR10 dataset into 300 clients, and choose $\{20\%, 40\%, 60\%, 80\%, 100\%\}$ clients in each round. We run algorithms for 200 communication rounds, and report the global accuracy on the round that achieves the best train accuracy.

Algorithm	0.2		0.4		0.6		0.8		1.0	
	Local	Global	Local	Global	Local	Global	Local	Global	Local	Global
FedAvg	29.22	31.10	29.61	29.43	30.63	31.17	30.46	29.03	30.28	30.47
IFCA	31.95	16.67	38.07	23.33	41.26	29.57	58.86	49.50	43.76	26.62
FeSEM	29.86	25.37	38.31	28.00	36.05	32.93	40.53	27.53	45.32	30.79
FedSoft	66.59	10.03	67.37	9.20	70.76	10.00	85.37	10.20	83.08	22.00
FedEM	52.65	36.17	51.75	32.23	52.81	44.87	52.44	47.17	51.31	43.35
FedConceptEM	61.33	62.10	62.02	64.2	65.24	65.07	63.97	63.90	62.74	63.83

Ablation studies on value of δ . We vary the value of δ as the threshold for removing models, and results in Figures 11 and 12 show that: 1) both FedConceptEM and FedConceptEM-Adam can find the true number of concepts. 2) FedConceptEM-Adam is more robust to δ , while γ_{ijk} in FedConceptEM converge slower as δ decreases. 3) FedConceptEM-Adam converges faster initially, but the final results are similar.

Table 5: **Ablation study on the number of concepts.** We split CIFAR10 dataset to 300 clients, and change the number of concepts to $[1, 3, 5]$, and initialize $[3, 3, 5]$ models respectively. We report the local and global accuracy on the round that achieves the best train accuracy for each algorithm.

Algorithm	1		3		5	
	Local	Global	Local	Global	Local	Global
FedAvg	53.63	61.90	30.28	30.47	18.55	16.54
FeSEM	53.25	48.00	45.32	30.79	26.84	17.96
FedEM	64.37	58.00	51.31	43.35	51.82	17.76
FedConceptEM	58.78	64.20	62.74	63.83	39.27	39.34

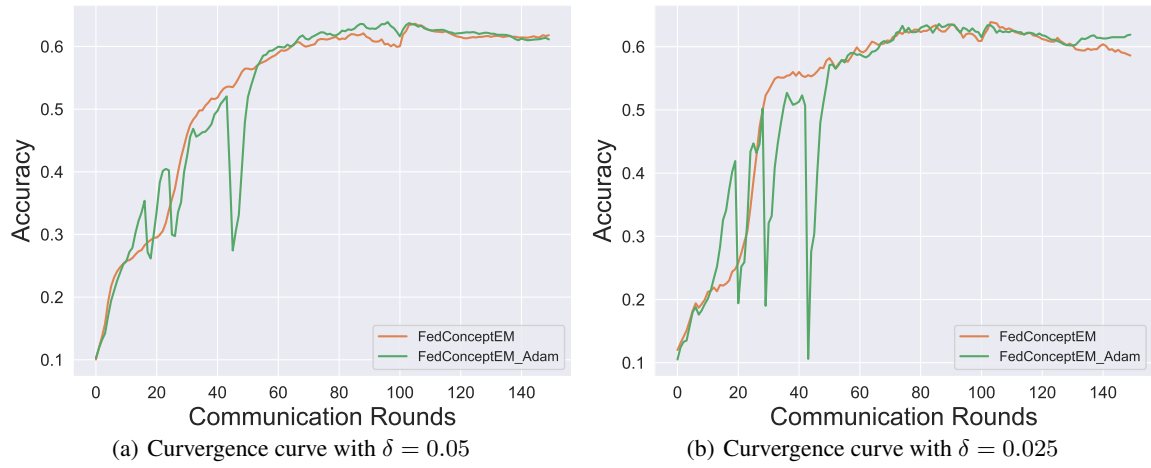


Figure 12: **Convergence curve of FedConceptEM and FedConceptEM-Adam with different δ .** We split CIFAR10 dataset to 300 clients, initialize 6 models, and report the convergence curve of FedConceptEM and FedConceptEM-Adam with $\delta = [0.05, 0.025]$. We use adaptive process, and models is removed to 3 as in Figure 11.